

Multiparametric MRI in detection and staging of prostate cancer

Lars Boesen

This review has been accepted as a thesis together with three previously published papers by University Copenhagen 31th of August 2014 and defended on 16th of January 2015

Tutor(s): Henrik S. Thomsen and Kari Mikines

Official opponents: Michael Borre, Jelle Bahrentz and Peter Iversen

Correspondence: Department of Urology and Urological Research, Herlev University Hospital, Herlev Ringvej 75, 2730 Herlev

E-mail: lars.boesen@dadlnet.dk

Dan Med J 2017;64(2):B5327

This PhD thesis is based on the three following papers:

Early experience with multiparametric magnetic resonance imaging-targeted biopsies under visual transrectal ultrasound guidance in patients suspicious for prostate cancer undergoing repeated biopsy.

Boesen L, Noergaard N, Chabanova E, Logager V, Balslev I, Mikines K, Thomsen HS.
Scand J Urol 2015;49;25-34

Prostate cancer staging with extracapsular extension risk scoring using multiparametric MRI: a correlation with histopathology

Boesen L, Chabanova E, Logager V, Balslev I, Mikines K, Thomsen HS.
Eur Radiol 2015;25;1776-85

Apparent diffusion coefficient ratio correlates significantly with prostate cancer Gleason score at final pathology

Boesen L, Chabanova E, Logager V, Balslev I, Thomsen HS.
J Magn Reson Imaging 2015;42;446-53

INTRODUCTION

Prostate cancer (PCa) is the second leading cause of cancer-related mortality and the most frequently diagnosed male malignant disease among men in the Nordic countries. Due to the introduction of prostate-specific-antigen (PSA) testing there has been a dramatic increase in the incidence of newly diagnosed PCa over the last 20-30 years. PCa is now detected at earlier stages causing stage-migration. The lifetime risk of a man being diagnosed with PCa is approx. 17% (one in six), but only 3-4% (one in thirty) will die of the disease supporting the fact that the majority of men with PCa never develop a clinical significant disease that will affect their morbidity or mortality [1]. However, despite

earlier detection of PCa, the mortality rate in Scandinavia has remained virtually unchanged and is one of the highest in the world. Thus, the manifestation of PCa ranges from indolent to highly aggressive disease. Due to this high variation in PCa progression, the diagnosis and subsequent treatment planning can be challenging. Active surveillance, surgery and radiation therapy are standard treatment options for men with localised or locally advanced disease. There is seldom just one right treatment choice and since surgery and radiation therapy may imply greater side effects such as impotence, incontinence and/or radiation damage to the bladder or rectum, it is essential to determine the exact tumour localisation, aggression and stage for optimal clinical management and therapy selection.

The current diagnostic approach with PSA testing and digital rectal examination followed by transrectal ultrasound biopsies lacks in both sensitivity and specificity in PCa detection and offers limited information about the aggressiveness and stage of the cancer. Recent scientific work supports the rapidly growing use of multiparametric magnetic resonance imaging (mp-MRI) as the most sensitive and specific imaging tool for detection, lesion characterisation and staging of PCa. Its use may improve many aspects of PCa management, from initial detection of significant tumours using mp-MRI-guided biopsies to evaluation of biological aggressiveness and accurate staging which can facilitate appropriate treatment selection. However, the experience with mp-MRI in PCa management in Denmark has been very limited. Therefore, we carried out this PhD project based on three original studies to evaluate the use of mp-MRI in detection, assessment of biological aggression and staging of PCa in a Danish setup with limited experience in mp-MRI prostate diagnostics. The aim was to assess whether mp-MRI could 1) improve the overall detection rate of clinically significant PCa previously missed by transrectal ultrasound biopsies, 2) identify patients with extracapsular tumour extension and 3) categorize the histopathological aggressiveness based on diffusion-weighted imaging.

BACKGROUND

Diagnosis of prostate cancer (PCa)

PCa is suspected by elevated PSA and/or an abnormal digital rectal examination (DRE) and the diagnosis is made by transrectal ultrasound-guided biopsies (TRUS-bx) [2].

PSA

PSA is a natural enzyme that is produced almost exclusively by the prostatic epithelial cells and is used as a serum marker for PCa. However, PSA is organ-specific, but not cancer-specific, as benign conditions such as benign prostatic hypertrophy (BPH), prostatitis and other urinary symptoms may cause elevated PSA levels.

There is no absolute PSA cut-off level that indicates PCa and there is no PSA level below which a man is guaranteed not to have PCa, although the risk of PCa is associated with higher levels of PSA [3]. Traditionally, a threshold level ≥ 4 ng/ml has been established as suspicious of PCa that trigger biopsies. However, at this cut-off level only about 1/3 men with elevated levels will in fact have cancer and "normal" levels may falsely exclude the presence of cancer, supporting the fact that PSA cannot be used to diagnose or exclude PCa [4–8]. The PSA level is also used in risk stratification of newly diagnosed PCa patients, included into predictive staging nomograms and for monitoring treatment response [2].

Digital rectal examination (DRE)

DRE is a fundamental part of the clinical examination of the patient where PCa feels hard and irregular when a tumour is palpable. The majority (70–75%) of PCa lesions are located in the peripheral zone and are therefore theoretically palpable over a certain size [9]. Still 25% of the tumours are located in the transitional zone, which cannot be reached by DRE due to the anatomical location. In addition, as PCa is now detected at earlier stages and at smaller tumour volumes, the number of palpable tumours is strongly reduced. This makes DRE lack in both sensitivity and specificity [10–13]. However, suspicious findings at DRE is a predictor for more pathologically aggressive prostate cancer [14,15] and is a strong indicator for performing prostate biopsies, as it allows for identification of 18% of men with PCa at "normal" PSA levels [15]. DRE is traditionally used for clinical tumour staging (cT category), for risk stratification and included into predictive staging nomograms.

Transrectal ultrasound (TRUS) and TRUS-bx

Transrectal ultrasound (TRUS) is the standard imaging modality for evaluating the prostate. As gold standard, the diagnosis of PCa is made by histological examination of 10–12 TRUS-bx cores from standard zones in the prostate [16]. The role of prostate biopsies has changed over the past decades from pure cancer detection to be an essential part of clinical management. TRUS is ideal for determining prostate gland volume and guiding the biopsy needle, but lacks in both sensitivity and specificity for detection and staging of PCa [16,17]. Most PCa lesions, if visualised on TRUS, appear hypo-echoic compared to the normal peripheral zone. However, PCa lesions are often difficult to see, as more than 40–50% of the cancerous lesions are iso-echoic [17,18] and cannot be identified. In addition, evaluation of the transitional zone on TRUS is very limited due to the heterogenic appearance often caused by BPH making detection of anteriorly located tumours particularly difficult. Therefore, there is a high risk that a tumour is either being missed or the most aggressive part of the tumour is not hit by the systematic standard biopsies (Figure 1a+b). This may lead to either repeated biopsies (re-biopsy) or an incorrect Gleason score (GS) and risk stratification. Conversely, multiple biopsies may hit a small clinically insignificant PCa micro-focus by chance and contribute to over-detection and increase the risk of over-treatment (Figure 1c).

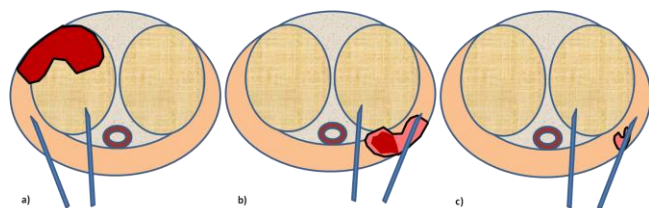


Figure 1: Standard TRUS-bx is a) missing a significant tumour (dark red area), b)

missing the most aggressive part of the tumour (dark red area) and c) an insignificant tumour (pink area) is hit by chance by the systematic biopsies.

Patients with persistent suspicion of PCa after TRUS-bx with negative findings pose a significant clinical problem due to the high false-negative rates of 20–30% [7,19–21]. This means that up to 30% of the patients with a normal TRUS-bx will in fact have cancer. To overcome this, patients with negative TRUS-bx often undergo several repeated biopsy procedures that will increase both biopsy-related costs and may contribute to increased anxiety and morbidity (e.g. infectious complications) among patients. Furthermore, multiple biopsies can cause inflammation and scar tissue that may hamper and complicate any subsequent surgical intervention if PCa is diagnosed. The detection rate at first TRUS re-biopsy is 10–22% [7,22] depending on the initial biopsy technique with decreasing rates at repeated procedures. Still a significant number of cancers are missed [20]. In order to increase the detection rate by TRUS-bx and to overcome the absence of target identification, some groups have extended the number of cores [23] and others are moving towards saturation biopsy techniques [24]. This approach may lead to an increased overall detection rate, but it may also increase the risk of detecting small insignificant well-differentiated tumours that potentially lead to unnecessary treatment [19,25,26]. The limitations of TRUS-bx have led to an intense need for an image modality that can improve the detection rate of clinically significant PCa without increasing the number of diagnosed insignificant tumours and optimally decrease the number of unnecessary biopsy sessions and cores. The prostate now remains the only solid organ where the diagnosis is made by "blind" biopsies scattered throughout the organ.

Grading PCa using Gleason score (GS)

The histopathological aggressiveness of PCa is graded by the GS [27,28]. The cancerous tissue is graded on a scale from 1–5 according to the histopathological arrangement and appearance of the cancerous cells. This discrepancy between the normal and cancerous tissue reflects the aggressiveness of the cancer (Figure 2).

ISUP Modified Gleason Grade

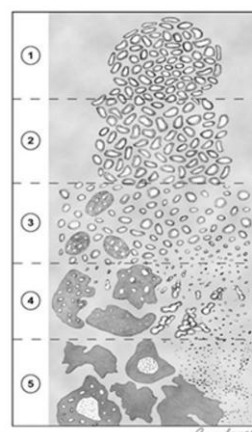


Figure 2: The modified Gleason grading system currently used for histopathological grading [29]. In lower Gleason grade 1 and 2, the cancerous tissue closely resembles normal prostatic tissue and the disparity increases with higher Gleason grades. (Reprinted with permission from the publisher).

As more than one class of Gleason grade can be present in the biopsy tissue, a composite GS (ranging from 2–10) combining 'the dominant' and 'the highest grade' is assigned. A Gleason grade ≥ 3 or a GS ≥ 6 is the cellular pattern most often used as the distinc-

tion of cancerous tissue. The GS assigned after radical prostatectomy differs as it is the sum of 'the most dominant' and 'the second most dominant' Gleason grade. The GS is strongly related to the clinical behaviour of the tumour and is a prognostic factor for treatment response. High GS implies increased tumour aggressiveness and increased risk of local and distant tumour spread with a worse prognosis [30–32]. Thus, it has been proposed to divide the GS into risk groups according to the risk of progression and metastasis [33]. However, the pre-therapeutic risk assessment of a patient with newly diagnosed PCa is based on the GS from TRUS-bx, which can be inaccurate due to sampling error, confirmed by the fact that the GS is upgraded in every third patient following radical prostatectomy [34]. Incorrect GS at biopsy may lead to incorrect risk stratification and possible over- or under-treatment. Furthermore, the reporting of GS has changed over time with broadening of the Gleason grade 4 criteria [35] in order to improve the correlation between biopsy and radical prostatectomy Gleason scores and to better stratify patients to predict clinical outcomes. This has resulted in a significant upgrade of tumour GS and made it difficult to compare pathological data over time.

Clinical staging of PCa

Clinical staging of PCa is based on the TNM classification [36]. The clinical tumour (cT) stage is based on 4 main categories (cT1–T4) with subgroups, describing the local extent of the tumour (Figure 3).

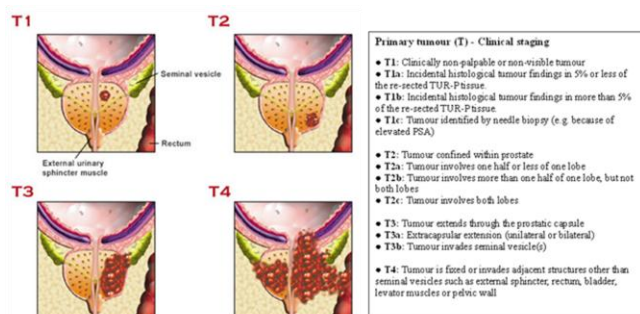


Figure 3: Clinical staging of PCa (cT1–T4) with subgroups. (Source: <http://www.prostatecancercentre.com/whatis.html>).

The prognosis and treatment selection of PCa is strongly related to cT stage at diagnosis. Especially, the distinction between localised (cT1–cT2) PCa and locally advanced disease (cT3–cT4) is essential when planning treatment strategies. DRE and TRUS are traditionally used for clinical staging of PCa. However, as DRE and TRUS lack in both sensitivity and specificity and often underestimate the size and stage of the cancer [16], the prediction of extra prostatic tumour extension (EPE) has low accuracy [37,38]. PSA also has limited accuracy in PCa staging as there is a significant overlap between PSA levels and tumour stage [39–41]. Nevertheless, the clinical results from DRE, TRUS-bx findings (including GS) and PSA values are used to stratify patients into risk groups (D'Amico)[42,43] (Table 1).

	cT stage	Gleason score	PSA
Low risk	cT1–T2a	≤6	<10
Intermediate risk	cT2b	7	10–20
High risk	≥cT2c	≥8	>20

Table 1: D'Amico risk groups based on cT stage, Gleason score and PSA.

The development of nomograms have increased the diagnostic accuracy of predicting EPE at final pathology and recurrence after prostatectomy [44–46]. However, the results are based on a statistical prediction integrating the known intrinsic sampling error of TRUS-bx and do not incorporate visual anatomic imaging that provides individual information about localisation, side and possible level of EPE.

Overall, PSA, DRE and TRUS-bx have several limitations regarding detection (Table 2), lesion characterisation and staging of PCa and there is a need for clinicians to base the therapeutic decision on more accurate imaging techniques.

Limitations for PCa detection	
PSA	A threshold of 4 ng/ml may miss significant cancer at lower values Low specificity leading to many unnecessary biopsies
DRE	Low sensitivity as most tumours are non-palpable
TRUS-bx	Low/moderate sensitivity and specificity for PCa detection Risk of missing significant tumours Risk of diagnosing insignificant tumours Multiple non-targeted biopsies are required Repeated biopsy procedures are necessary Increased risk of infectious complications and inflammation with multiple biopsies Possible sampling error leading to incorrect diagnosis of tumour volume, extent and GS Under-sampling of the anterior region

Table 2: Main limitation with the current diagnostic modalities for PCa detection.

MRI OF THE PROSTATE

MRI of the prostate is performed on either a 1.5 or 3.0 Tesla MRI scanner combined with a pelvic-phased-array coil (PPA-coil) placed over the pelvis with or without an endorectal coil (ERC) depending on the clinical situation. The use of an ERC can enhance image quality, as it is located in the rectum just posterior to the prostate gland as well as fixate the prostate during the examination, which might reduce motion artefacts. However, the disadvantages of the ERC are increased scan time, increased costs and reduced patient compliance due to the location of the coil in the rectum. The additional image quality of the ERC is valuable on 1.5 T MRI, whereas it is more questionable on 3.0 T. Due to the increased spatial resolution (the ability to separate two dense structures from each other) and the increased signal-to-noise ratio on 3.0 T MRI, the majority of prostatic MRI examinations can be performed with acceptable image quality without an ERC. Although, studies have shown improved image quality and diagnostic performance with an ERC at 3.0 T [47,48], the topic is still under debate and several centres reserve the use of an ERC only for staging purposes if possible extra-prostatic disease is decisive for the treatment plan. The European Society of Urogenital Radiology's (ESUR) MR prostate guidelines states that the use of an ERC is optional for detection and preferable for staging at 3.0 T MRI [49].

The MRI image quality is also depending on patient preparation. The administration of an oedema prior to the examination and an injection of an intestinal spasmolyticum may diminish rectal

peristaltic motion and reduce the intra-luminal air that may cause artefacts on MRI.

Multiparametric MRI (mp-MRI)

The development of mp-MRI offers new possibilities in detection, lesion characterisation and staging of PCa due to its high resolution and soft-tissue contrast. Published data [49–53] supports the rapidly growing use of mp-MRI as the most sensitive and specific diagnostic imaging modality for PCa management. Mp-MRI can provide information about the morphological, metabolic and cellular changes in the prostate as well as characterise tissue vascularity and correlate it to tumour aggressiveness (Gleason score) [54,55].

Multiparametric MRI sequences

Mp-MRI includes high-resolution anatomical T2-weighted (T2W) and T1-weighted (T1W) images in combination with one or more functional MRI techniques such as diffusion-weighted imaging (DWI) and dynamic contrast enhanced (DCE) imaging [49]. Proton MR-spectroscopic imaging (MRSI) can be used in addition to the other MRI techniques and responds to the changes in tissue metabolism that typically occurs in PCa. It can be used to distinguish cancer from benign tissue [56] and provide information about lesion aggressiveness [57]. However, MRSI is technically challenging and requires high expertise and longer scan time often combined with the use of an ERC, so many centres do not incorporate MRSI in their standard protocol. The ESUR MR prostate guidelines do not list MRSI as a requirement for prostate examination, which is why it is not included in the mp-MRI protocol used in this PhD study.

T1-weighted imaging (T1W)

T1W imaging is used in conjunction with T2W imaging to detect post-biopsy haemorrhage and to evaluate the contour of the prostate and the neurovascular bundles. T1W imaging cannot be used to assess the intra-prostatic zonal anatomy due to its low spatial resolution. Post-biopsy haemorrhage can mimic PCa on T2W imaging, as both cancerous lesions and haemorrhage can appear as dark hypo-intense areas. It has been reported to occur in 28-95% of patients [58–60]. However, only haemorrhage will appear as an area with high signal intensity on T1W imaging and can be used to rule out false-positive findings on T2W imaging [59] (Figure 4a+b).

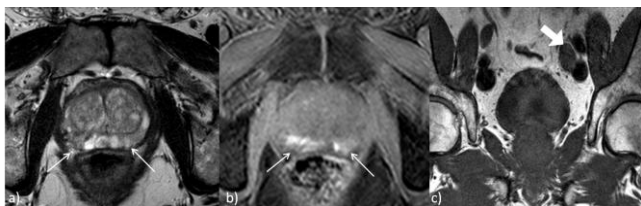


Figure 4: Peripheral zone haemorrhage (white arrows) causes a) hypo-intense areas on axial T2W imaging and b) high signal intensity on pre-contrast axial T1W imaging. T1W coronal imaging with increased field of view (c) reveals an enlarged lymph node by the left iliac vessels (thick white arrow).

It has been shown that the extent of haemorrhage is lower in a PCa lesion than in the adjacent benign tissue [58] and the presence of "the excluded haemorrhage sign" on T1W imaging in conjunction with an area of homogenous low signal intensity on T2W imaging is highly accurate for PCa detection [60]. In addition, T1W imaging with increased field of view can also be used to detect enlarged lymph nodes or signs of metastatic disease in the pelvic region (Figure 4c).

T2-weighted imaging (T2W)

High-resolution T2W imaging is the cornerstone in every prostate MRI. T2W imaging with high spatial resolution provides a good overview of the prostatic zonal anatomy and it allows for detection, localisation and staging of PCa. The peripheral zone often appears with high signal intensity due to the high content of water in the glandular tissue opposed to the transitional- and central zone that often have lower signal intensity (Figure 5). The transitional- and central zone is often referred in combination as "the central gland", as the two zones may be difficult to distinguish on MRI. However, awareness about the location and appearance of the central zone is important as its manifestation may imitate PCa resulting in a false-positive reading on MRI (Figure 5b). However, PCa may rarely occur in the central zone, but when it does, it is typically more aggressive [61].

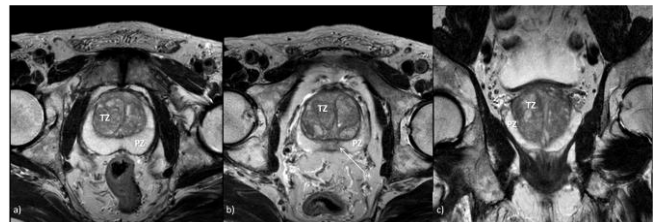


Figure 5: Normal prostate anatomy. T2W images show the peripheral zone (PZ) and transitional zone (TZ) in the a) axial and c) coronal plane. Axial T2W image at the prostatic base (b) shows the central zone (white arrow) as a hypo-intense area surrounding the ejaculatory ducts.

The prostatic capsule appears as a thin fibro-muscular fringe of lower signal intensity surrounding the prostate. PCa in the peripheral zone typically appears as a round or oval area of low signal intensity in contrast to the higher signal intensity from the homogeneous benign peripheral zone [62,63] (Figure 6). However, some PCa lesions can be iso-intense on T2W imaging and cannot be seen.



Figure 6: T2W imaging of a PCa lesion in the left peripheral zone (white arrow) on a) axial b) sagittal and c) coronal view. (Source [52]. Reprinted with permission from the publisher).

PCa occurring in the transitional zone is not as distinctly outlined as it often has lower and mixed signal intensities due to BPH nodules that may interfere with interpretation and mimic PCa. An area of homogeneous low signal intensity and usually anteriorly located with a lenticular shape are features of PCa occurring in the transitional zone [64] (Figure 7).

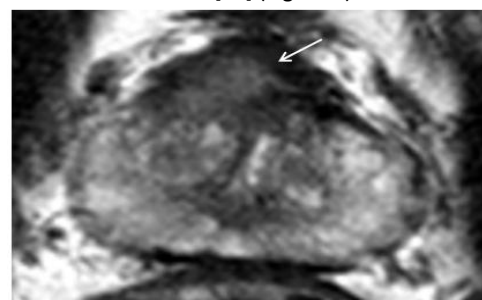


Figure 7: Axial T2W image of a PCa lesion in the right anterior part of the prostate (white arrow).

It has been shown that the degree of signal intensity on T2W imaging is related to the Gleason score as cancers with a Gleason grade 4 or 5 tend to be more hypo-intense than Gleason grade 3 [65]. Also the growth pattern of the cancer may affect the appearance where “sparse” tumours with increased intermixed benign prostatic tissue appear more like “normal” peripheral zone than more dense tumours [66]. Moreover, there are several benign conditions in the prostate (e.g. haemorrhage, atrophy, BPH, calcifications and prostatitis) that also can appear as an area of low signal intensity on T2W imaging causing false-positive readings. A meta-analysis reported an overall sensitivity and specificity of 0.57-0.62 and 0.74-0.78 for PCa localisation using T2W imaging alone [67]. Due to this moderate sensitivity and specificity, T2W imaging should be combined with additional functional MRI techniques such as DWI and DCE imaging to increase the diagnostic performance.

PCa staging is accompanied by determination of possible EPE (T3-T4 disease). T2W imaging is the dominant MRI modality for assessment of extracapsular extension (ECE) and seminal vesicle invasion (SVI), where direct signs of ECE can be visualised as tumour growth outside the prostatic capsule and into the periprostatic tissue. Secondary, indirect signs of ECE include bulging or loss of capsule, neurovascular bundle-thickening, capsular irregularity, thickening or retraction, obliteration of the recto-prostatic angle and abutment of tumour. Similarly, signs of seminal vesicle invasion (SVI) include expansion of tumour from the prostatic base into the SV, with low T2W-signal intensity in the lumen, filling in of angle and possible concomitant enhancement (DCE imaging) and/or impeded diffusion (DWI) [49,68–71] (Figure 8)

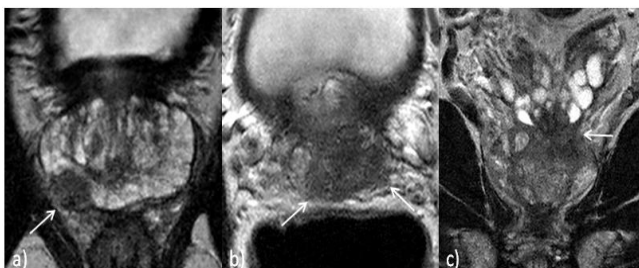


Figure 8: T2W imaging of PCa (white arrows) in a) the right peripheral zone with direct sign of extracapsular extension and b+c) tumour involvement of the seminal vesicles.

Diffusion-weighted imaging (DWI)

DWI is a non-invasive functional MRI technique that assesses changes in diffusion of water molecules due to microscopic structural changes. By applying different diffusion-weighted gradients (b-values) to the water protons in the tissue, DWI generates different signal intensities that quantify the movement of free water molecules. Normal prostatic tissue, especially the peripheral zone, contains glandular structures where water molecules can move freely without restriction. PCa often depletes the glandular structures and contains more tightly packed cells causing restricted diffusion. Changes in diffusion are reflected in changes in the signal intensity on DWI where areas with restricted diffusion will be bright on DWI. DWI is usually performed with different b-values where low b-values (0-100) predominantly represent

a signal decay caused by the perfusion in the tissue, whereas higher b-values represent water movement in the extra- and intracellular compartment [72]. The use of DWI provides both qualitative and quantitative information about the tissue cellularity and structure that can be used for lesion detection and characterisation. Therefore, a qualitative assessment of an area with high signal intensity on high b-value DWI often represents an area with restricted diffusion caused by tightly packed cells. The apparent diffusion coefficient (ADC) is calculated based on the signal intensity changes of at least two b-values to quantitatively assess the degree of diffusion restriction. The calculation of ADC is performed using built-in software in the MRI scanner or workstation. An ADCmap is generated based on the ADC value in each voxel of the prostate. Restriction of diffusion causes a reduction in the ADC value and is dark on the ADCmap [72,73]. PCa typically has higher cellular density and restricted diffusion compared to the surrounding normal tissue. Therefore, PCa lesions are often bright on high b-value DWI and dark on the ADCmap with lower ADCtumour values [73–76]. Thus, DWI can help in the differentiation between malignant and benign prostatic tissue and the use of DWI in the diagnosis of PCa has been proven to add sensitivity and especially specificity to T2W imaging alone [67,77] (Figure 9).

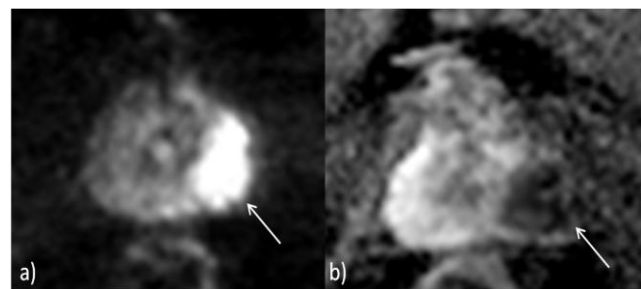


Figure 9: DWI of PCa in the left peripheral zone (white arrow) on a) axial b1400 b) axial ADCmap corresponding to the same tumour in Figure 6. (Source [52]. Reprinted with permission from the publisher).

Studies have shown an inverse correlation between the mean ADCtumour value calculated from the cancerous lesion on the ADCmap and the GS [55,78–82] signifying that ADCtumour values can be used as a non-invasive marker of tumour aggression. Attempts have been made to define specific cut-off values to separate malignant from benign tissue and to further differentiate between GS groups. However, due to different study methodologies with different b-values, different MRI equipment and field strengths along with patient variability between studies, a wide range and inconsistency in mean ADCtumour values have been reported [78,80,83,84]. Furthermore, there is a considerable overlap between ADC values from malignant and benign tissue [85,86] and a wide variability depending on the zonal origin [87,88]. Thus, there is no consensus on absolute ADCtumour cut-off values corresponding to different GS.

Dynamic contrast enhanced MRI (DCE-MRI)

DCE-MRI utilises the fact that malignant and benign prostatic tissues often have different contrast enhancement profiles. DCE-MRI analysis is based on changes in the pharmacokinetic features of the tissue mainly due to angiogenesis. DCE-MRI consists of a series of fast high-temporal (the ability to make fast and accurate images in rapid succession) T1W images before, during and after a rapid intravenous injection of a gadolinium-based contrast agent. The prostatic tissue is generally highly vascularised, making

a simple assessment of pre- and post-contrast images inadequate for PCa characterisation [89]. PCa often induces angiogenesis and increased vascular permeability compared to normal prostatic tissue [90,91] resulting in a high and early contrast enhancement peak (increased enhancement) followed by a rapid washout of the contrast [92–95] (Figure 10).

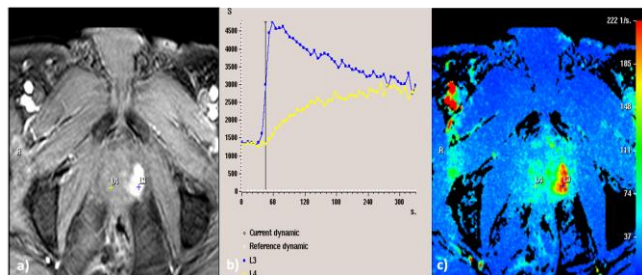


Figure 10: DCE-MRI of PCa in the left peripheral zone corresponding to the same tumour in Figure 6 + Figure 9. The a) dynamic contrast enhanced T1W image and the c) corresponding DCE colour map show early focal contrast enhancement in the tumour (red area). b) The dynamic DCE-curve L3 (blue) is a typical malignant curve (curve type 3) with a high peak, rapid early enhancement (high wash-in rate) and early wash-out. The DCE-curve L4 (yellow) is from a non-malignant region with no early wash-out (curve type 1). (Source [52]. Reprinted with permission from the publisher).

There are several methods to describe the pharmacokinetic features in the tissue. Qualitatively by a visual characterisation of the enhancement curves, quantitatively by applying complex pharmacokinetic models to determine the contrast exchange rate between different cellular compartments or semi-quantitative by calculating various kinetic parameters of the enhancement curves - wash-in/wash-out rate, time to peak etc. In addition, various post-processing software tools are used to analyse and describe the DCE-MRI including overlaid colourised enhancement maps that can be used to identify pathological changes and PCa. A detailed description of the analysis of DCE-MRI can be read in the review by Verma et al.[94].

Previous studies have verified that DCE-MRI in conjunction with other MRI modalities can increase the diagnostic accuracy of PCa detection [94,96–98] and may even improve the detection of ECE [99]. The use of DCE-MRI primarily adds sensitivity to the mp-MRI performance and is essential for detection of local recurrence [100–104]. However, a recent study by Baur et al. [105] found that DCE-MRI did not add significant value to the detection of PCa. DCE-MRI lack in specificity as benign conditions, such as hyper-vascularised BPH nodules and prostatitis can mimic pathological enhancement patterns [94,106]. Thus, DCE-MRI is best analysed in conjunction with other MRI modalities such as T2W imaging and DWI to achieve optimum sensitivity and specificity for PCa assessment.

Clinical guidelines and Prostate Imaging Reporting and Data System (PIRADS):
The basic principle of a scoring system for mp-MRI readings is to identify abnormal regions and grade each region according to the degree of suspicion of PCa based on the appearance on the mp-MRI. However, prostate mp-MRI interpretation is challenging and has a steep learning curve where experienced readers are significantly more accurate than non-experienced readers [107–109]. The diagnostic accuracy of mp-MRI differs among previously published studies [110–113] partly due to different study protocols, diagnostic criteria, MRI equipment and expertise, which have led to a debate about mp-MRI’s readiness for routine use

[114]. Mp-MRI has been criticised for the lack of standardisation and a uniform scoring system. Clinical guidelines [49] have therefore recently been published to promulgate high-quality mp-MRI acquisition and evaluation. The guidelines are based on literature evidence and consensus expert opinions from prostate MRI experts from ESUR and include clinical indications for mp-MRI and a structured uniform Prostate Imaging Reporting and Data System (PIRADS) to standardise prostatic mp-MRI readings. The PIRADS classification is a scoring system for prostate mp-MRI similar to the BIRADS for breast imaging. It is based on the five-point Likert scale and should include 1) a graphic prostate scheme with 16-27 regions 2) a separate PIRADS score for each individual lesion and 3) a max. diameter measure of the largest lesion. All MRI modalities - e.g. T2W, DWI and DCE imaging – are scored independently (1-5) on a five-point scale for each suspicious lesion within the prostate and the summation of all individual scores (ranging 3-15 for 3 modalities) constitute the PIRADS summation score. In addition, each lesion is given a final overall score (ranging 1-5) according to the probability of clinically significant PCa being present (Table 3).

Score	Criteria	SI=signal intensity
T2W imaging for peripheral zone		
1	Uniform high SI	
2	Linear, wedge-shaped or geographic area of low SI, usually not well-demanded	
3	Intermediate appearances not in categories 1/2 or 4/5	
4	Discrete, homogeneous low-signal focus/mass confined to the prostate	
5	Discrete, homogeneous low SI focus with ECE/invasive behaviour or mass effect on the capsule (bulging), or broad (>1.5 cm) contact with the surface	
T2W imaging for transitional zone		
1	Heterogeneous transition zone adenoma with well-defined margins: “organised chaos”	
2	Areas of more homogeneous low SI, however, well-margined, originating from the transitional zone/BPH	
3	Intermediate appearances not in categories 1/2 or 4/5	
4	Areas of homogeneous low SI, ill defined: “erased charcoal drawing sign”	
5	Same as 4, but involving the anterior fibro-muscular stroma sometimes extending into the anterior horn of the peripheral zone, usually lenticular or water-drop shaped	
Diffusion-weighted imaging (high b-value images ~ ≥b800)		
1	No reduction in ADC compared to normal glandular tissue. No increase in SI on high b-value images	
2	Diffuse hyper SI on high b-value images with low ADC; no focal features, linear, triangular or geographical features allowed	
3	Intermediate appearances not in categories 1/2 or 4/5	
4	Focal area(s) of reduced ADC but iso-intense SI on high b-value image	
5	Focal area/mass of hyper SI on the high b-value images with reduced ADC	
Dynamic contrast enhanced imaging		
1	Type 1 enhancement curve	
2	Type 2 enhancement curve	
3	Type 3 enhancement curve	
+1	Focal enhancing lesion with curve types 2-3	
+1	Asymmetric lesion or lesion at an unusual place	

Overall final score

1	Clinically significant disease is highly unlikely to be present
2	Clinically significant disease is unlikely to be present
3	Clinically significant disease is equivocal
4	Clinically significant disease is likely to be present
5	Clinically significant disease is highly likely to be present

Table 3: PIRADS classification for T2W, DWI and DCE imaging [49]. Since there is considerable different anatomical appearance between the peripheral- and transitional zone on T2W imaging, different PIRADS criteria are applied for the two zones. Illustrative examples of the PIRADS criteria for the MRI modalities are seen in reference [115,116].

Extra prostatic tumour extension (EPE)

In addition to the PIRADS classification, each lesion should also be assessed for possible EPE. The ESUR MR prostate guidelines list a table of mp-MRI findings with a corresponding risk score stratified into different EPE criteria with concomitant tumour characteristics/findings (Table 4).

Criteria	Findings	Score
Extracapsular extension (ECE)	Abutment	1
	Irregularity	3
	Neurovascular bundle thickening	4
	Bulge, loss of capsule	4
	Measurable extracapsular disease	5
Seminal vesicles (SVI)	Expansion	1
	Low T2 signal	2
	Filling in of angle	3
	Enhancement and impeded diffusion	4
Distal sphincter	Adjacent tumour	3
	Effacement of low signal sphincter muscle	3
	Abnormal enhancement extending into sphincter	4
Bladder neck	Adjacent tumour	2
	Loss of low T2 signal in bladder muscle	3
	Abnormal enhancement extending into bladder neck	4

Table 4: EPE risk scoring of extra prostatic extension [49].

ECE and/or SVI corresponds to locally advanced T3-disease and invasion into the bladder neck, external distal sphincter, rectum and/or side of the pelvic wall are considered T4-disease, although only the first two T4-findings are included in the ESUR EPE risk scoring.

Anatomical T2W imaging is the dominant MRI modality for EPE assessment. However, some of the categories (e.g. SVI) also include findings on functional imaging (enhancement and impeded diffusion ~ risk score 4). It is recommended that suspicion of EPE should be given an overall score ranging 1-5 according to the probability of EPE being present. Therefore, the five-point scale is considered a continuum of risk with higher scores corresponding to higher risk of EPE. However, not all categories include the total scoring range 1-5 and e.g. functional imaging findings are not included in the assessment of ECE. Previous studies show that functional imaging may improve detection of ECE [99,117,118], especially for less experienced readers [108]. Therefore, the interpretation and overall impression of possible ECE may be influenced by personal opinion when incorporating functional imaging finding.

Overall, the combination of morphological T2W imaging with functional sequences in a multiparametric approach, preferably on a high-field MRI (e.g. 3T) with or without an endorectal coil depending on the clinical situation, has shown that mp-MRI can increase the diagnostic accuracy in detection, characterisation and staging of PCa [97,119–123]. Thus, mp-MRI has the ability to change the management of PCa [51].

OBJECTIVES AND HYPOTHESIS

The main objective of this PhD study is to investigate the use of multiparametric MRI in detection and staging of PCa in a Danish setup and to assess if multiparametric MRI can

- Improve the overall detection rate of clinically significant PCa previously missed by transrectal ultrasound biopsies

- Identify patients with extracapsular tumour extension and

- Categorize the histopathological aggressiveness based on diffusion-weighted imaging.

The secondary purpose is to gain experience in the use of multiparametric MRI for PCa management in Denmark. This experience may form the basis for the future – using multiparametric MRI as a diagnostic adjunct in selected patients, as practiced at international leading PCa MRI centres.

This thesis is based on the following hypotheses:

1. Multiparametric MRI can improve the detection rate of clinically significant PCa in patients with persistent suspicion after TRUS-bx with negative findings by adding multiparametric MRI-targeted biopsies towards suspicious lesions.

2. Multiparametric MRI-targeted biopsies allow for a more accurate Gleason grading.

3. Multiparametric MRI is an accurate diagnostic technique in determining PCa clinical tumour stage and ECE at final pathology.

4. Multiparametric MRI with diffusion-weighted imaging can be used to assess the Gleason score of PCa tumours.

The use of multiparametric MRI in detection of metastasis (lymph nodes or bone) and potential recurrence - locally or distant - falls outside the scope of this thesis.

SPECIFIC PART

This thesis is based on 3 original studies using mp-MRI as a diagnostic tool in the detection, assessment of biological aggression and staging of PCa. Each study is introduced with introductory remarks and described briefly in the following part and in more detail in the individual manuscripts in the appendix.

All studies were approved by the Local Committee for Health Research Ethics (No.H-1-2011-066) and the Danish Data Protection Agency and were conducted as single institutional studies. The studies were registered at Clinicaltrials.gov (No.NCT01640262). All patients were included prospectively and written informed consent was provided.

The mp-MRI examination protocol was the same for all patients in all three studies using two 3.0 T MRI scanners (Achieva/Ingenia, Philips Healthcare, Best, the Netherlands) with a PPA-coil (Philips Healthcare, Best, the Netherlands) positioned over the pelvis. If tolerated, a 1 mg intramuscular Glucagon (Glucagon®, Novo Nordisk, Bagsvaerd, Denmark) injection combined with a 1 mg Hyoscinebutylbromid (Buscopan®, Boehringer Ingelheim, Ingelheim am Rhein, Germany) intravenous injection were administered to the patients to reduce peristaltic motion. Tri-planar T2W images from below the prostatic apex to above the seminal vesicles were obtained. In addition, axial DWI including 4 b-values (b0, b100, b800 and b1400) along with reconstruction of the corresponding ADCmap (b-values 100 and 800), together with DCE images before, during and after intravenous administration of 15 ml gadoterate meglumine (Dotarem 279.3 mg/ml, Guerbet, Roissy CDG, France) were performed. The contrast agent was administered using a power injector (MedRad, Warrendale, Pennsylvania, USA) followed by a 20 ml saline flush injection at a flow rate of 2.5 ml/s. For imaging parameters see Table 5.

	Pulse sequence	TR (ms)	TE (ms)	FA (°)	FOV (cm)	ACQ matrix	Number of slices	Thickness (mm)
Axial DWI, b= 0,100,800, 1400 s/mm ²	SE-EPI	4697 / 4916	81 / 76	90	18x18	116x118 / 116x118	18/25	4
Axial T2w	SE-TSE	3129 / 4228	90	90	16x16 / 18x18	248x239 / 248x239	20/31	3
Sagittal T2w	SE-TSE	3083 / 4223	90	90	16x16 / 16x20	248x242 / 268x326	20/31	3
Coronal T2w	SE-TSE	3361 / 4510	90	90	19x19	252x249 / 424x423	20	3
Coronal T1w	SE-TSE	675 / 714	20 / 15	90	40x48 / 44x30	540x589 / 408x280	36/41	3.6 / 6
Axial 3d DCE	FFE-3d-TFE	5.7 / 10	2.8 / 5	12	18x16	128x111 / 256x221	18	4 / 4.5

SE = spin echo, EPI = echo planar imaging, TSE = turbo spin echo, TFE = turbo field echo, FFE = fast field echo, TR = repetition time, TE = echo time, FA = flip angle, ACQ matrix = acquisition matrix.

Table 5 : Sequence parameters for 3.0 Tesla Achieva/Ingenia multiparametric MRI with PPA-coil.

Study I: Early experience with multiparametric magnetic resonance imaging-targeted biopsies under visual transrectal ultrasound guidance in patients suspicious for prostate cancer undergoing repeated biopsy

Introductory remarks

It is evident that TRUS-bx for PCa detection is prone to sampling error [7,19,20], most often caused by the absence of a target identification. To overcome the lack in sensitivity and specificity for TRUS-bx, patients with prior negative TRUS-bx findings and persistent suspicion of PCa frequently undergo several repeated biopsy (re-biopsy) procedures, and still a significant number of cancers are missed [20]. Similarly, the GS from TRUS-bx can be inaccurate, confirmed by the fact that the GS is upgraded in every third patient following radical prostatectomy. These limitations in TRUS-bx have led to an intense need for a way to improve the detection and localisation of clinically significant PCa. As previously stated, mp-MRI of the prostate seems to have the potential to solve the problem [49–53,124]. Studies show that it is feasible to target biopsies towards the most aggressive part of suspicious lesions seen on mp-MRI and thereby improve the detection rate of clinically significant PCa [125–131] and achieve a more accurate Gleason grading [54,132]. However, mp-MRI has never been

applied at our institution for PCa detection and for guiding targeted biopsies towards mp-MRI-suspicious lesions prior to this study. The patient population and results represent our first initial experience with this new technique.

Aim

To investigate the detection rate of PCa by mp-MRI-targeted biopsies in patients with prior negative TRUS-bx findings without preceded experience for this and to evaluate the clinical significance of the detected cancers.

Material and methods

Patients scheduled for repeated biopsies were prospectively enrolled. Inclusion criteria required that all patients had a history of negative TRUS-bx findings and a persistent suspicion of PCa based on either PSA value, an abnormal DRE or a previous abnormal TRUS-image. The exclusion criteria were patients previously diagnosed with PCa or contraindication to mp-MRI (pace-maker, magnetic implants, severe claustrophobia, previous moderate or severe reaction to gadolinium-based contrast media, impaired renal function with GFR<30 ml/min). Mp-MRI was performed prior to the biopsies and analysed for suspicious lesions. All identified lesions were registered on a 18-region prostate diagram (Figure 11) and scored according to the PIRADS classification given a sum of scores (ranging 3-15) [49].

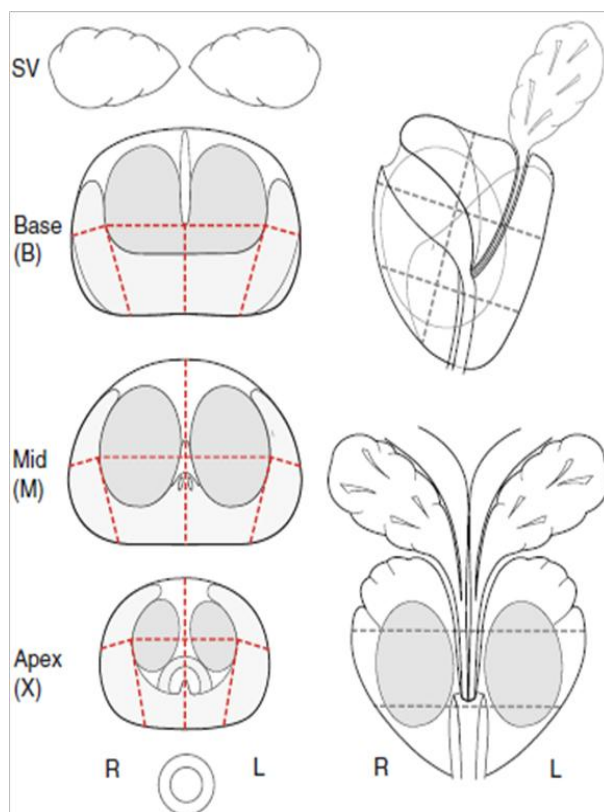


Figure 11: The prostate is divided into 12 posterior and 6 anterior regions. (Reprinted with permission from the publisher [133,134]).

Additionally, each lesion was classified overall on a Likert five-point scale according to the probability of clinically significant malignancy being present. The PIRADS and Likert scores were separately divided into 3 risk groups (high, moderate and low) according to suspicion of PCa.

Initially, all patients underwent repeated standard TRUS-bx (10 cores) (Figure 12) blinded to any mp-MRI findings.

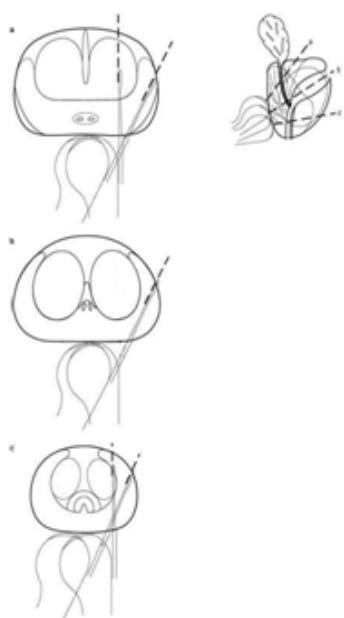


Figure 12: Axial and sagittal scheme of our standard ten TRUS-biopsy cores performed with an end-fire probe. The biopsy cores extend approximately 17-20 mm from the prostatic rectal surface into the prostate. The biopsies are taken from a) base – lateral/medial b) mid-gland – lateral and c) apex – lateral/medial. (Modified and reprinted with permission from the publisher [135]).

The standard biopsies were followed by visual mp-MRI-targeted biopsies (mp-MRI-bx) under TRUS-guidance of any mp-MRI-suspicious lesion considered not to be hit on the systematic TRUS-bx (Figure 13).

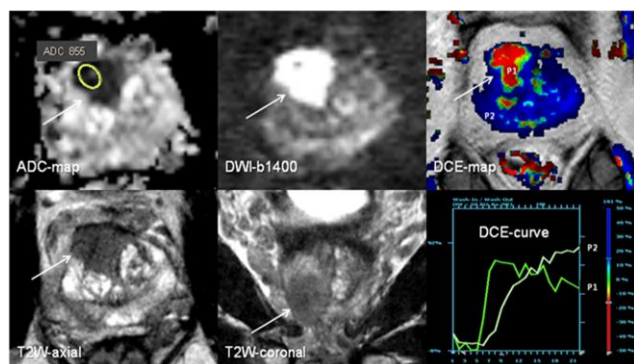


Figure 13: Mp-MRI (T2W, DWI and DCE imaging) shows a tumour suspicious region in the anterior part of the prostate (white arrows) that is considered not to be hit by the systematic TRUS-bx. The region is hypo-intense on T2W imaging, dark on the ADCmap (ADCtumour value 855 ($\times 10^{-6} \text{mm}^2/\text{sec}$)) and bright on the DWI-b1400 indicating a solid tumour mass. The corresponding DCE colour map shows focal enhancement in the region (red area) and the dynamic DCE-curve (P1) is a typical malignant (type 3) curve with rapid early enhancement and early wash-out. The DCE-curve (P2) is from a non-malignant region. The region was classified as high suspicion of prostate cancer (PIRADS summation score 5-5-5, overall Likert score 5).

Main results

Eighty-three patients with a median of 2(1-5) prior negative TRUS-bx sessions and median PSA of 11(2-97) underwent mp-MRI before re-biopsy. PCa was found in 39/83 (47%) patients using TRUS- and mp-MRI-bx. There was a total of 156 identified lesions ranging from low to highly suspicious giving a median of 2 (0-5) per patient. Biopsies were positive for PCa in 52/156 (33%) mp-MRI identified lesions and mp-MRI identified at least one lesion

with some degree of suspicion in all 39 patients diagnosed with PCa. Both the PIRADS summation score and the overall Likert classification showed a high correlation with biopsy results ($p < 0.0001$). Five patients (13%) had cancer detected only on mp-MRI-bx outside the systematic biopsy areas ($p = 0.025$) and another 7 patients (21%) had an overall GS upgrade of at least one grade ($p = 0.037$) based on the mp-MRI-bx. Secondary PCa lesions not visible on mp-MRI were detected by TRUS-bx in 6/39 PCa patients. All secondary lesions were GS 6(3+3) tumour foci in 5-10% of the biopsy core. No patients had a GS upgrade based on positive TRUS-bx from non-visible lesions on mp-MRI. Two patients had insignificant PCa detected providing an overall detection rate of clinically significant PCa of 45% (37/83 patients) among which 27% (10/37) harboured high-grade (GS ≥ 8) cancer.

Conclusion

Multiparametric MRI before repeated biopsy even without preceded experience can improve the detection rate of clinically significant PCa by combining standard TRUS-bx with mp-MRI-targeted biopsies under visual TRUS-guidance and it allows for a more accurate Gleason grading.

Study II: Prostate cancer staging with extracapsular extension risk scoring using multiparametric MRI: a correlation with histopathology

Introductory remarks

Local staging of PCa plays an important role in treatment planning and prediction of prognosis. It is evident that DRE and TRUS do not have the ability to correctly localise and stage the extension of the cancer, thus prediction of ECE has low accuracy [2,37,38]. Radical prostatectomy (RP) provides great disease control for patients with localised PCa (cT1-T2), while RP for locally advanced disease (cT3) remains controversial [2,136]. Preoperative accurate knowledge of tumour stage and possible ECE are crucial in achieving the best surgical, oncological and functional result. Mp-MRI has emerged as a sensitive and specific image modality for PCa staging and prediction of ECE at final pathology [51]. However, the diagnostic accuracy differs among studies [107,111,113,137,138]. Previous studies (including study I in this thesis) have validated the PIRADS classification for PCa detection and localisation using both targeted biopsies [139–141] and RP specimen [142] as standard reference, but the ESUR MR prostate guidelines also recommend a five-point risk scoring for possible EPE. This study represents our experience using the ESUR MR prostate guidelines scoring of extra prostatic disease focusing on ECE risk scoring in the preoperative evaluation of PCa staging.

Aim

To evaluate the diagnostic accuracy of preoperative multiparametric MRI with ECE risk scoring in the assessment of prostate cancer tumour stage and prediction of ECE at final pathology.

Material and methods

Patients with clinically localised PCa (cT1-T2) determined by DRE and/or TRUS and scheduled for RP were prospectively enrolled. All patients underwent mp-MRI (T2W, DWI and DCE imaging) prior to RP and all lesions were evaluated according to the ESUR MR prostate guidelines' PIRADS classification and scoring of extra prostatic disease focusing on the ECE criteria. The images were evaluated by two readers with different experience in mp-MRI interpretation. An mp-MRI T-stage (cTMRI) and an ECE risk score

were assigned. Additionally, suspicion of ECE was dichotomised into either organ-confined (OC) disease or ECE based on tumour characteristics and personal opinion incorporating functional imaging findings. All patients underwent RP and the histopathological results served as standard reference and were compared to the mp-MRI findings in the assessment of T-stage and ECE.

Results

Eighty-seven patients with median age 65 (range 47-74) and a median PSA 11 (range 4.6-45) underwent mp-MRI before RP. The correlation between cTMRI and pT showed a spearman rho correlation of 0.658 ($p < 0.001$) and 0.306 ($p = 0.004$) with a weighted kappa of 0.585 [CI 0.44;0.73] and 0.22 [CI 0.09;0.35] for reader A and reader B, respectively. The prevalence of ECE after RP was 31/87 (36%). ECE risk scoring showed an AUC of 0.65-0.86 on the ROC-curve for both readers and a sensitivity, specificity and diagnostic accuracy of 81% [CI 63;93], 78% [CI 66;88] and 79% at the best cut-off level (risk score ≥ 4) for the most experienced reader. When tumour characteristics were influenced by personal opinion and functional imaging, the sensitivity, specificity and diagnostic accuracy for prediction of ECE changed to 74% [CI 55;88], 88% [CI 76;95] and 83% for reader A and 61% [CI 0.42;0.78], 77% [CI 0.64;0.87] and 71% for reader B, respectively.

Conclusion

Multiparametric MRI with ECE risk scoring by a dedicated reader is an accurate diagnostic technique in determining prostate cancer tumour stage and ECE at final pathology.

Study III: Apparent diffusion coefficient ratio correlates significantly with prostate cancer Gleason score at final pathology

Introductory remarks

The histopathological aggressiveness of PCa is graded by the GS and is strongly related to the tumours' clinical behaviour. High GS implies increased tumour aggressiveness and risk of local and distant tumour spread with a worse prognosis. However, the majority of men diagnosed with PCa often harbour a non-aggressive low GS tumour focus that seldom develops into a clinical disease that will affect the morbidity or mortality. The GS from TRUS-bx that is used for pre-therapeutic classification of tumour aggressiveness can be inaccurate due to sampling error. Incorrect GS at biopsy may lead to incorrect risk stratification and possible over- or under-treatment. Thus, there is a need to improve the pre-therapeutic assessment of true GS. Previous studies show that cancerous tissue has lower DWI-calculated ADCTumour values than benign prostatic tissue (ADCbenign) and that there is a negative correlation with the GS. However, there is an inconsistency due to different study methodologies with a wide variability in reported ADCTumour values corresponding to different GS. To overcome some of this variability, we hypothesise that the ADCratio (defined as the ADCTumour divided by the ADCbenign value) might be more useful and predictive in determining true GS, as it may level out some of the variation. This study represents our experience using ADC measurements (ADCTumour and ADCratio) in the assessment of the GS.

Aim

To evaluate the association between the ADCTumour and the ADCratio calculated from pre-operative diffusion-weighted MRI

with the GS at final pathology and to determine the best parameter for this.

Material and methods

Patients with clinically localised PCa scheduled for RP were prospectively enrolled from study II. Diffusion-weighted MRI was performed prior to RP as part of the diagnostic workup in study II and mean ADCTumour values on the ADCmap from all identified malignant tumours were measured. All patients underwent RP and all tumour foci ≥ 5 mm in the longest dimension were outlined by the pathologist on a cross-sectional diagram and selected for comparison with mp-MRI. Using the histopathological map as a reference, the ADCbenign value was obtained from a non-cancerous area to calculate the ADCratio. The ADC measurements were correlated with the GS from each selected tumour foci from the prostatectomy specimen.

Results

Seventy-one patients with a median age of 65 (range 47-73) and a median PSA of 10.6 (range 4.6-46) underwent mp-MRI before RP. There were a total of 104 (peripheral zone=53, transitional zone=51) separate tumour foci identified on histopathology and were selected for comparison. There was a statistical significant difference ($p < 0.001$) between mean ADCTumour and mean ADCbenign values and between mean ADCTumour values of tumours originating in either the peripheral- or transitional zone. There was no significant difference ($p = 0.194$) in mean ADCratio between the two zones.

The association between ADC measurements and GS showed a significantly negative correlation ($p < 0.001$) with spearman rho for ADCTumour (-0.421) and ADCratio (-0.649), respectively. There was a statistically significant difference between both ADC measurements and the GS groups for all tumours ($p < 0.001$). The difference remained significant for mean ADCratio when stratified by zonal origin, but not for mean ADCTumour for tumours located in the transitional zone ($p = 0.46$). ROC-curve analysis showed an overall AUC of 0.73 (ADCTumour) to 0.80 (ADCratio) in discriminating Gleason 6 from Gleason $\geq 7(3+4)$ tumours. The AUC remained virtually unchanged at 0.72 (ADCTumour), but increased to 0.90 (ADCratio) when discriminating Gleason $\leq 7(3+4)$ from Gleason $\geq 7(4+3)$.

Conclusion

Preoperative ADC measurements showed a significant correlation with tumour GS at final pathology. The ADCratio demonstrated the best correlation compared to the ADCTumour and radically improved accuracy in discriminating GS $\leq 7(3+4)$ from GS $\geq 7(4+3)$ tumours.

DISCUSSION

This PhD thesis evaluates the use of mp-MRI in the detection, assessment of biological aggression and staging of PCa in a Danish setup. In this section, the main study results will be discussed and compared to previous research with a reflection on clinical use, general limitations and finally future perspectives. More detailed discussions of specific study results and limitations are part of the main articles in the appendix.

Detection: Initial diagnosis and prostate biopsy

The indication for performing prostate biopsies is driven by non-specific and non-sensitive tests such as elevated PSA and/or an

abnormal DRE assuming that the patient might have PCa. As TRUS also lacks in both sensitivity and specificity in PCa detection, 10–12 "screening" biopsy cores are taken systematically from the peripheral zone scattered throughout the prostate hoping to hit the possible cancer, including the most aggressive part. The accuracy of TRUS-bx in PCa detection varies widely between studies, especially due to inter-operator variation, various biopsy techniques and often a poor discrimination of a specific PCa target on TRUS. The low diagnostic yield of TRUS-bx often leads to repeated biopsy sessions.

In study I, we demonstrated that pre-biopsy mp-MRI for detection of PCa in patients with prior negative TRUS-bx findings can improve the overall detection rate by adding mp-MRI-bx under visual TRUS-guidance to standard TRUS-bx even without preceded experience for doing this. We found an overall PCa-detection rate of 47% (39/83) in patients with a median of 2 prior negative TRUS-bx sessions among which 26% (10/39) harboured high-grade PCa (GS \geq 8). According to the literature, the detection rate at first TRUS re-biopsy is 10–22% [7,22] depending on the initial biopsy technique with decreasing rates at repeated procedures. Only two patients had insignificant PCa providing an overall detection rate of clinically significant PCa of 45% (37/83 patients). We concluded that suspicious lesions seen on mp-MRI can be targeted by biopsies and improve the detection rate of clinically significant PCa, which is in line with previous studies [125–131]. In our setting, 5/39 (13%) patients had PCa detected only by mp-MRI-bx and another 7/34 (21%) patients had an overall GS upgrade cumulating to a total of 12/39 (31%) newly diagnosed PCa patients that may have had their prognosis and treatment management altered due to the use of mp-MRI as an adjunct to TRUS-bx.

There are different ways of performing targeted biopsies of mp-MRI-suspicious lesions. In study I we used visual fusion with cognitive targeting, where the mp-MRI-suspicious lesions are visually matched and registered on the corresponding axial TRUS-image based on zonal anatomy and tissue landmarks. The physician performing the TRUS uses the mp-MRI findings to select an appropriate TRUS-region for a targeted biopsy. The overall PCa detection rate in study I is in accordance with previous findings as outlined in the review by Lawrentschuk et al. [127], although they find a higher proportion of PCa detected purely by the mp-MRI-targeted biopsy cores. Our high PCa detection rate of 41% (34/83) using standard end-fire biopsies alone can be explained by the fact that not all patients included in the study had the initial TRUS-bx performed at our institution. Patients are often referred to our department for repeated biopsies, as TRUS-bx is limited to a very few highly experienced operators using an end-fire biopsy probe unlike many of the referring departments where TRUS-bx is practiced widely by all urologists using a side-fire probe. The end-fire probe allows for better sampling of the lateral and apical regions of the prostate at standard biopsies where PCa often resides [143] (Figure 12) Mp-MRI-bx is particularly good at detecting anteriorly located tumours that are frequently missed by TRUS-bx [144–146], which is confirmed in this study where more than 70% of the mp-MRI PCa-positive lesions were located in the anterior or apical region (Figure 1study I). It is our experience that the end-fire biopsy needle is essential for targeting mp-MRI-suspicious lesions as it enters the prostatic surface more perpendicularly and penetrates deeper and more anteriorly into the prostate facilitating better sampling of the apical and anterior regions. This is confirmed in a recent study by Ploussard et al. [147] showing increased detection rate of PCa in highly-suspicious MRI lesions using an end-fire- compared to a side-fire-approach.

However, despite a rather surprisingly high PCa detection rate at standard endfire TRUS-bx, we still found a significant improvement in the detection rate ($p=0.025$) and GS upgrading ($p=0.037$) by adding mp-MRI-bx as an adjunct to our standard TRUS-bx.

Visual translation of the mp-MRI image onto the greyscale TRUS-image cannot always be accurate. In eight mp-MRI-suspicious lesions (Figure 2study I), we experienced that the targeted mp-MRI-bx were negative for PCa compared to the standard cores obtained from the same prostatic region. This could be caused by the intentional dispersion of the two biopsies, but it is more likely caused by translation error. There will be a margin of error, when the operator has to visually correlate the mp-MRI image onto a real-time 2D TRUS image and translate it all into a 3D representation of the prostate, especially if the prostate is large or the lesion is located anteriorly [124]. Methods for improving the accuracy of the targeted biopsies have recently been developed. Fusion software has enabled a co-registration between the mp-MRI data and real-time TRUS imaging. Fusion of the two modalities (MR-TRUS) allows a lesion that is marked on the mp-MRI to be transferred onto the real-time TRUS images and identified during the TRUS-procedure. Mp-MRI-bx can then be targeted towards the marked lesion [115,126,132,139,148–153] with potentially increased accuracy.

Using TRUS as guidance for mp-MRI-bx, either cognitive- or software-based, gives the operator the advantage of adding mp-MRI-bx to the systematic standard biopsies, which is still the recommended standard approach [2]. However, there will always be a possible misregistration, when combining two image modalities. In-bore direct MRI-guided biopsies within the MRI suite is possible due to the development of increased speed in MRI imaging, MRI compatible instruments and advanced visualisation software with tools to guide and verify needle placement. Several studies have been published using both 1.5 T [154,155] and 3.0 T [128,156–160] MRI with good results and summarised in a recent review by Overduin et al. [161]. Using in-bore mp-MRI-bx, Hambrook et al. [156] found a PCa detection rate of 59% among which 93% cancers were clinically significant in a patients cohort with 2 previous negative TRUS-bx sessions using an average of 4 biopsy cores per patient. Similar results were later confirmed by the same group [128] and also investigated in men without previous prostate biopsies [159].

Although, performing biopsies directly in the MRI suite seems to be the most accurate technique, the biopsy procedure can be time-consuming, as well as the diagnostic MRI and the biopsy procedure need to be performed in two different sessions. Some also report that the biopsy device has limited reach, especially towards the base of the prostate [162].

The diagnostic performance of mp-MRI in PCa detection and localisation is depending on the tumour size, GS, histological architecture and location [163]. Low-volume (<0.5 ml) and low-grade (GS 6) tumours are less likely to be identified compared to higher grade (GS \geq 7) and larger tumours [164–166], whereas detection of tumours \geq 1 ml does not seem to be affected by the GS [164]. Thus, mp-MRI is not as sensitive in detecting insignificant PCa. Therefore, if only identified mp-MRI-suspicious lesions are targeted by biopsies, the chance of detecting insignificant PCa foci is reduced. Haffner et al.[135] compared this "targeted-only" strategy against extended systematic TRUS-bx (12 cores) for detection of significant PCa in 555 patients undergoing initial biopsy and used the same targeted-biopsy technique with visual/cognitive mp-MRI/TRUS-fusion as we did in study I. By using

this "targeted-only" biopsy approach, only 63% of the referred patients with clinical suspicion of PCa required subsequent biopsies using a mean of 3.8 cores per patient (compared to 12 standard cores). In addition, the diagnosis of 13% insignificant cancers was avoided. These findings were recently confirmed by Pokorný et al. [159] in 223 consecutive biopsy-naïve men with elevated PSA showing that the mp-MRI "targeted-only" approach can reduce the detection of low-risk PCa and reduce the number of men requiring biopsy while improving the overall detection rate of intermediate/high-risk PCa.

The location of the PCa lesion affects the sensitivity and specificity of mp-MRI. Transitional-zone tumours are more difficult to identify, as reported by Delongchamps et al. [167] where sensitivity and specificity decreased from 80% and 97% in the peripheral zone, to 53% and 83% in the transition zone. In addition, sparse tumours where PCa growth is intermixed with normal tissue can also limit the diagnostic performance of mp-MRI in detection of PCa [66].

PCa aggressiveness and ADC measurements

The GS is the most widely used method of grading the histopathological aggressiveness of PCa and it is the most important prognostic factor for treatment response. Several predictive and prognostic tools for risk stratification and counselling have been introduced for optimal clinical management and therapy selection [42,46,168–174]. However, they are all based on the GS from TRUS-bx, which can be substantially discordant with the true GS verified after radical prostatectomy. This lack of ability to confidently identify low-grade tumours at biopsy is one of the reasons for the current issue with overtreatment. Hence, improving the pre-therapeutic assessment of GS may increase the accuracy of the predictive and prognostic tools and improve the risk stratification when planning individualised treatment strategies. In study III, we demonstrated that preoperative DWI-calculated ADC measurements (ADCTumour value and ADCratio) showed a significant correlation with tumour GS at final pathology. As reported by others [55,78], we also found that decreasing mean ADCTumour values were associated with higher GS groups. A retrospective study by Hambrook et al. [79] found a significant inverse correlation between ADCTumour values and GS for tumours originating in the peripheral zone and Jung et al. [81] showed that the same holds true for transitional zone tumours. When comparing previous studies, a wide range in mean ADCTumour values has been reported [78–81,84] with a substantial overlap corresponding to different GS groups. To overcome some of this variability, we hypothesised that the ADCratio might be more useful and predictive in determining true GS, as it may level out some of the variation since the ADCratio is not only related to the ADCTumour value, but also to the individual prostate's unique signal characteristics. We found that decreasing mean ADCratio values (increased difference between ADCTumour and ADCbenign) were associated with higher GS groups and demonstrated a superior correlation to GS compared to the ADCTumour value. Previous studies have had similar results calculating the prostate ADCratio for better correlation with GS. Vargas et al. [80] found a significant inverse correlation with GS using both ADCTumour value and ADCratio and Thörmer et al. [175] showed a high discriminatory power (AUC=0.90) of normalised ADC (equivalent to ADCratio) between low- and intermediate/high-risk cancer. This was recently confirmed by Lebovici et al. [176] concluding that the ADCratio may be more predictive of tumour grade than analysis based on ADCTumour values alone. However, the study was relatively small (n=22 patients) and had prostate biopsies as

reference standard. Conversely, Rosenkrantz et al. [177] did not find any benefit of using normalised ADC compared to the ADCTumour value in terms of AUC for differentiating benign from malignant tissue in the peripheral zone.

Mp-MRI using DWI-calculated ADCmaps may improve patient management by targeting biopsies towards areas suspicious of harbouring the most aggressive part of the tumour and thereby improving prediction of true GS to facilitate better risk stratification. Although not addressed as a specific endpoint in study I, we found that 7/34 (21%) PCa patients had an overall GS upgrade due to the use of additional mp-MRI-bx. The GS was upgraded from low- to intermediate/high-grade cancer in 5/7 patients. Similarly, a prospective study by Siddiqui et al. [132] including 582 patients showed an overall GS upgrade in 32% using additional mp-MRI-bx. The targeted biopsies detected 67% more GS ≥ 7 (4 + 3) tumours than systematic TRUS-bx alone and missed 36% of GS ≤ 7 (3 + 4) tumours, thus increasing the detection ratio of high/low-grade cancer. However, definitive pathology from RP was not available. Using DWI/ADC-guided biopsies, Hambrook et al. [54] correctly identified true GS at final pathology in 88% compared to 55% using standard TRUS-bx. The risk of DWI/ADC-guided biopsies mistakenly underscored an area with a Gleason grade 4- or 5 component, as a Gleason grade 3, was less than 5%. The ADCmap may also facilitate PCa detection and localisation. Watanabe et al. [178] used the ADCmap and ADCTumour value to prospectively stratify 1448 consecutive biopsy-naïve patients into two groups (with or without low ADC lesions). All patients underwent systematic biopsies and the low ADC-lesion group had additional targeted biopsies of the low ADC lesions. The PCa detection rate was highest in the targeted biopsy group and PPV of the mp-MRI findings was 70%-90% depending on anatomical lesion location.

A great benefit in improving the pre-therapeutic assessment of GS is the ability to separate low-risk (GS 6) from intermediate/high-risk (GS ≥ 7) cancer. We found an overall AUC of 0.75 for the ADCTumour value in differentiating low-risk GS 6 tumours from intermediate-/high-risk GS ≥ 7 (3+4) tumours. This lies within the AUC levels (0.72-0.76) reported by others [78,179], although higher AUC values have been reported [79]. The AUC increased to 0.81 for the ADCratio indicating improved accuracy. This ability to discriminate low-risk from intermediate/high-risk tumours is important in a clinical situation, as it is often decisive of the treatment selection. As more and more PCa patients are detected in an earlier stage, there will be an increase in both significant and insignificant tumours. A major challenge is to correctly assess the aggressiveness of the cancer to determine appropriate treatment to prevent morbidity and mortality. Patients with localised prostate cancer with low tumour burden may be candidates for active surveillance (AS) depending on the clinical situation. AS includes close monitoring with PSA, DRE and repeated biopsies. This regimen is to avoid over-treatment of cancers that are found to be insignificant at diagnosis and therefore not likely will affect patient morbidity and mortality. It is crucial that these patients are staged and risk-stratified correctly, so tumour characteristics are not underestimated, and patients with more advanced disease mistakenly are put in AS instead of having active treatment. Mp-MRI with ADC measurements can be used to assess PCa aggressiveness as an adjunct to other clinical parameters such as PSA kinetics and tumour stage in the selection and follow-up of patients undergoing AS regimens [82,180–183]. Furthermore, mp-MRI can be incorporated into nomograms and improve the prediction of insignificant cancer [184]. Mp-MRI may reveal early signs of clinically significant disease and poor prognostic features

such as larger tumour volumes or high-grade tumours, especially in the anterior region [185], potentially missed by TRUS-bx [183]. Additional targeted biopsies towards the suspicious regions can be performed along with a possible re-evaluation of the treatment plan. Conversely, a normal/low suspicious mp-MRI can confirm the absence of significant PCa, due to its high negative predictive value, thus AS can be implemented. AS is traditionally reserved for patients without Gleason grade 4- or 5 tumours. However, it has been addressed that because of the increased reporting of Gleason grade 4 since the ISUP GS modification in 2005 [27], a low percentage of Gleason grade 4 should not necessarily lead to immediate exclusion of the AS regimen [186]. This, combined with the recent findings showing low-volume Gleason grade 4 on needle biopsy is associated with low-risk tumour at radical prostatectomy [187], makes the differentiation between GS 7(3+4) and GS 7(4+3) clinically important. In study III, the overall AUC of the ADCtumour value did not change when discriminating between $GS \leq 7(3+4)$ and $GS \geq 7(4+3)$. However, the AUC of the ADCratio changed radically to 0.90 indicating a high clinical value of this ADC parameter.

Although, we found a significant difference between the mean ADC measurements and the GS groups in study III, there was still a considerable overlap between the groups. Due to this heterogeneity, a definite cut-off value for separating the GS groups could not be made. DWI largely reflects the average amount of "fluid" within the tissue as an indirect "glandular ratio". However, the GS is also influenced by other factors such as cellularity, glandular/cell size and shape, the appearance of the inter-glandular space and other intermixed histological components, which are included in the overall pathological assessment of the GS. Moreover, the aggressiveness of PCa is not only determined by its histological GS. Other factors such as PSA, tumour volume, location and extension including possible EPE have to be taken into account in risk stratification of the patients. Thus, clinical staging of PCa plays an essential part when planning patient-tailored management

Clinical staging of PCa

Radical prostatectomy (RP) provides great disease control for patients with localised PCa (cT1-T2), while RP for locally advanced disease (cT3) remains controversial [16,188]. Preoperative accurate knowledge of tumour stage and possible ECE is crucial in achieving the best surgical, oncological and functional result. The pre-therapeutic local staging of PCa and prediction of ECE by DRE and TRUS have low accuracy [37,38]. Accurate pre-therapeutic staging of PCa implies appropriate estimation of tumour volume, location and possible EPE. The diagnostic accuracy of mp-MRI staging differs among previous studies [107,111,113,137,138] partly due to different study protocols, diagnostic criteria, MRI equipment and expertise. In study II, we found a significant correlation between the tumour stage estimated by mp-MRI (cTMRI) and the pathological specimen pT) for the most experienced reader with a Spearman $\rho=0.658$ ($p<0.001$) and moderate to good agreement using weighted kappa=0.585. Complete agreement between cTMRI and the pathological stage is difficult to obtain, as mp-MRI does not identify all the small dispersed insignificant tumour foci that frequently are present within the prostate and are incorporated into the overall evaluation and reporting of the pathological stage. This can easily cause a discrepancy between a T2a/T2b stage identified on mp-MRI and a T2c stage reported at pathology for organ-confined (OC) tumours. However, the exact stage differentiation among OC tumours is of less importance, as patients with OC disease often can receive poten-

tially curative surgery regardless of the T2-stage. In contrast, the treatment selection of PCa strongly relies on the identification of patients with ECE.

In study II, we demonstrated that multiparametric MRI with ECE risk scoring by a dedicated reader is an accurate diagnostic technique in determining tumour stage and ECE at final pathology. The prevalence of ECE at histopathology was 36% in patients with pre-therapeutic clinically localised PCa confirming the fact that DRE and TRUS often underestimate the tumour extension and stage. Mp-MRI using both ECE risk scoring and personal opinion for prediction of ECE at final pathology showed a diagnostic accuracy of 79-83% with a sensitivity and specificity ranging between 74-81% and 78-88% for the most experienced reader. These findings are in accordance with previous studies. A meta-analysis from 2002, covering a time period of 17 years by Engelbrecht et al. [110] that also included studies conducted in the early period of prostate MRI, reported a combined sensitivity and specificity of 71% in distinguishing between T2- and T3-disease on 1.5 T MRI systems. More recent studies at 3.0 T ERC MRI from experienced prostate-MRI experts report higher rates with sensitivity and specificity of 80-88% and 95-100%, respectively [47,189]. Although, we did not directly measure tumour volume in study II, other studies have found a good correlation between the estimated tumour volume on mp-MRI and the tumour volume from the radical prostatectomy specimen, especially for tumours ≥ 0.5 ml [164,190–192]. Identifying the "index" tumour in particularly has a prognostic significance [193,194]. Clinicians commonly use PSA levels, clinical stage - determined by DRE and/or TRUS - and biopsy GS combined in nomograms to predict pT stage at RP. We did not compare preoperative mp-MRI against predictive nomograms in study II, as the objective was to evaluate the diagnostic accuracy, as a single parameter in the assessment of tumour stage and prediction of ECE using the ECE risk score. However, mp-MRI has been found to perform significantly better than nomograms, DRE and TRUS in visualising the intra-prostatic tumour localisation and possible ECE including predicting the final pT-stage [44,137,184,195–198].

In recent years, mp-MRI has emerged as the most sensitive and specific imaging tool for PCa staging [51]. T2W imaging is the dominant MRI modality for staging and EPE evaluation due to its high spatial resolution for anatomical assessment. However, the use of functional imaging, e.g. DCE-MRI in conjunction with T2W imaging may improve staging performance [99], especially for less experienced readers [108]. This is also confirmed in our study II, where inclusion of personal opinion and functional imaging findings to T2W ECE tumour characteristics gave a slight increase in the diagnostic accuracy for prediction of ECE for both readers. Accurate staging and assessment of EPE using DWI is challenging due to lower spatial resolution and increased risk of image artefacts compared to T2W imaging. However, higher diagnostic accuracy in the diagnosis of SVI using DWI in conjunction with T2W imaging have been reported [199,200]. Similarly, recent studies have reported higher diagnostic accuracy using DWI at 3.0 T MRI in conjunction with T2W imaging regarding the diagnosis of ECE, compared to T2W imaging alone [117,118]. Thus, mp-MRI with T2W, DWI and DCE imaging is recommended in the ESUR MR prostate guidelines for staging [49].

Besides PCa lesion location and staging, mp-MRI can also provide additional information regarding prostate size, presence of a median lobe or the occurrence of larger vessels surrounding the prostate for patients undergoing RP. Improved staging performance may also reveal possible tumour involvement of the neurovascular bundles (NVB) and aid in the selection of patients

suitable for NVB preservation or a wider local resection [201,202]. In addition to local staging, regional lymph nodes and part of the pelvic bones can also be evaluated on the mp-MRI images depending on the MRI field of view.

Mp-MRI scoring using PIRADS and ECE risk scoring

Different interpretative approaches for mp-MRI have been evaluated in the literature [203]. For instance, Pinto et. al. [148] suggested that each MRI modality is characterised as either positive or negative in a binary approach where the summation of positive sequences graded the suspicion of PCa. Others have often used a variation of the five-point Likert scale to give an overall impression of the level of suspicion [190]. Recently, the PIRADS classification [49] was developed to provide a structured uniform algorithm for mp-MRI prostate interpretation and reporting. The PIRADS score can either be reported as the summation of all individual scores (ranging 3-15) or converted into an overall final score (ranging 1-5) similar to the Likert five-point scale. In study I, we used both the PIRADS summation score and the overall Likert scoring system to analyse suspicious lesions and found a highly significant correlation between positive biopsies and lesion suspicion on mp-MRI ($p < 0.001$). All but one low-suspicious PCa lesion and all missed secondary PCa lesions on mp-MRI were GS 6(3+3). These findings underline the potential value of using pre-biopsy mp-MRI to increase the detection rate of clinically significant PCa previously missed by standard TRUS-bx and to stratify the patients and lesions according to suspicion on mp-MRI using both the PIRADS summation score and the overall five-point Likert scale. The clinical value of the PIRADS summation score is validated in a recent prospective study by Portalez et al. [139] in a contemporary patient cohort in relation to repeated prostate biopsies. Using PIRADS summation score ≥ 9 as threshold, the authors report a sensitivity and specificity of 69% and 92%, respectively, and more interestingly a negative predictive value (NPV) of 95%. This high NPV can predict the absence of cancer with high confidence and thereby possibly reduce the number of unnecessary repeated biopsies in patients with low PIRADS scores. In study I, we validated both the PIRADS summation score and overall Likert score according to biopsy results. Rosenkrantz et al. [142] recently confirmed the good diagnostic performance in PCa localisation in a retrospective analysis using both scoring systems with RP specimen as reference standard, although the performance was better with Likert scoring for transitional tumours. Other groups have also validated the PIRADS classification for lesion detection and characterisation and found a good association between suspicion on mp-MRI and PCa [105,115,204]. In the PIRADS summation score, all mp-MRI modality scores are weighted equally. However, not all modalities are always equal in determining the presence of clinically significant PCa. For instance, DWI has been reported to be the best sequence for lesion detection in the peripheral zone [205] and conversely T2W imaging in the transitional zone [144]. Thus, there may be a "dominating" modality depending on the location of the lesion. Therefore, an overall final score ranging 1-5 (equivalent to the overall Likert score) that includes the interpretation of all individual scores, but driven by the dominant modality might better represent the "true suspicion score". Furthermore, there is an on-going debate about the necessity of including DCE imaging in the recommended minimum requirements in the ESUR MR prostate guidelines for PCa detection, as it may not add significant value to T2W imaging and DWI [105] to improve transitional zone cancer detection and localisation compared to T2W imaging alone [144]. Furthermore, DCE imaging is not as reliable for detecting transitional zone

tumours, as there is a significant overlap with hyper-vascular BPH findings [85]. However, DCE imaging seems to have the ability to aid in the differentiating between the normal central zone and PCa based on the enhancement curves [206], as the appearance of the central zone on T2W imaging and DWI have many features that may mimic PCa. Moreover, DCE imaging is still recommended for staging purposes and it is essential for detection of local recurrence [49].

The ESUR MR prostate guidelines also recommend scoring of extraprostatic disease on a five-point risk scoring scale. In study II, we validated this risk scoring focusing on ECE corresponding to locally advanced T3a-disease. Although, the ESUR MR prostate guidelines also recommend individual scoring of SVI (T3b) and bladder neck/distal sphincter involvement (T4-disease), we did not include these parameters in our study, as we considered the a priori probability of any patient in our population with clinically localised PCa having SVI, distal sphincter- or bladder neck involvement to be too low to validate a five-point risk scoring scale. The ECE risk scoring in study II showed an AUC of 0.65-0.86 on the ROC-curve indicating a high clinical value for the experienced reader with a sensitivity, specificity and diagnostic accuracy of 81%, 78% and 79% at the optimal risk score cut-off level ≥ 4 . When using a five-point scale, the ECE score is considered a continuum of risk with higher scores corresponding to higher risk of ECE. As the ECE risk scoring in the guidelines only evaluates tumour characteristics on T2W imaging and assigning a preoperative cTMRI staging requires a definitive decision on possible ECE and SVI, the suspicion of ECE was dichotomised into either organ-confined disease or ECE based on the established ECE-tumour characteristics and personal opinion incorporating functional imaging (DWI and DCE imaging) findings. By doing this, the diagnostic accuracy increased for both readers (71%-83%) and changed sensitivity and specificity to 74% and 88% for the most experienced reader and 61% and 77% for the less experienced reader in predicting ECE at final pathology.

The sensitivity and specificity of the mp-MRI reading can be affected by the way the physician weigh the image findings, especially when deciding on possible ECE in the equivocal cases. Until recently, RP was restricted to patients with localised PCa while patients with high suspicion of ECE and/or SVI were referred for radiation therapy. This might influence the physician to value high specificity with a low number of false-positive readings, so no patients with equivocal mp-MRI findings would be ruled out of possible curative surgery. However, there has been an increasing interest in performing RP in selected patients with locally advanced T3 disease with good results [207-210]. This may increase the interest in high-sensitive mp-MRI readings in order to direct the surgeon to the site of possible ECE to avoid positive surgical margins. Therefore, the mp-MRI ECE risk score threshold for ECE might be altered depending on the clinical situation. Furthermore, previous studies show that mp-MRI findings can be combined with clinical findings and nomograms and increase the overall pre-therapeutic diagnostic staging accuracy [44,184]. The reader performance of two readers with different experience in mp-MRI prostate interpretation was evaluated in study II. Overall, the most experienced reader A had a significantly higher performance than reader B in the assessment of ECE using both ECE risk scoring and personal opinion and was more accurate in predicting the pathological stage. Furthermore, our results indicate that the overall interpretation of possible ECE in our hands should not only rely on the ESUR MR prostate guidelines' ECE risk scoring in its current form, but whenever possible also incorporate functional imaging, especially for less experienced readers. It

is evident, that mp-MRI interpretation has a considerable learning curve and is a specialised task that requires substantial dedication and experience to allow for acceptable diagnostic results [107,211]. It has been proven that the diagnostic accuracy in detection of PCa increase significantly [212] through a dedicated prostate mp-MRI-reader education program and the difference in diagnostic accuracy between the readers in our study II indicates that the same also applies to our mp-MRI staging performance.

Limitations

Not all patients are suitable for mp-MRI due to absolute/relative contraindications such as a non-MRI compatible pacemakers, magnetic implants, severe claustrophobia as well as previous moderate or severe reactions to gadolinium-based contrast media for DCE-MRI imaging. Also very large patients may not fit inside the MRI tube. In our studies, we used a PPA coil positioned over the pelvis and lower abdomen. In some patients with significant abdominal obesity, we experienced movement artefacts caused by the synchronised respiratory movement of the PPA-coil. The use of an additional ERC could possibly be advantageous in these cases. High-quality images can only be obtained if the patient is able to lie perfectly still while the images are being recorded. Peristaltic rectal motion and intra-luminal rectal air may cause movement artefacts, but can be reduced by the administration of an oedema prior to the examination and/or an injection of an intestinal spasmolyticum. The presence of a hip replacement or other metallic objects near the prostate can also cause severe artefacts, especially on DWI.

Each MRI modality - T2W, DWI and DCE imaging - has its own clinical value and limitations and should be viewed as complementary to each other to balance sensitivity and specificity for optimal interpretation. Hypo-intense signals on T2W imaging in the peripheral zone can be caused by various benign conditions such as prostatitis, atrophy or supporting tissue and even the appearance of the central zone at the base of the prostate. The addition of DCE imaging and DWI to T2W imaging adds sensitivity and specificity to PCa detection and lesion characterisation. BPH nodules in the transitional zone can have almost identical appearances as PCa lesions with hypo-intensity, restricted diffusion and early enhancement. Asymmetry, unusual topography and homogenous low signal on T2W imaging are signs of PCa. However, sparse tumours with fine low-density trabeculae infiltrating benign prostatic tissue can hardly be distinguished from healthy tissue regardless of the use of additional functional imaging. In tumour staging, the ability to detect minimal ECE is often limited. Staging accuracy and determination of ECE require high spatial resolution [47,49,213], which is why the use of an ERC is recommended by the ESUR MR prostate guidelines [49] as part of the optimal requirements. However, with a tendency towards more aggressive surgical treatment of locally advanced T3-disease, the exact differentiation between organ-confined PCa and minimal ECE probably becomes less important, unless it is a matter of neuro-vascular bundle preservation.

Another major limitation with mp-MRI is the presence of post-biopsy haemorrhage, that can compromise the examination performance [59] and may persist for up to 6-8 weeks or even longer [58,214]. The exact timeframe of how long the post-biopsy changes persist is not accurately known and is probably highly individual from one patient to another. A general consensus on the time interval between biopsy and mp-MRI has therefore not been reached. Moreover, one retrospective study suggests not to

wait as the haemorrhagic changes do not influence on staging performance [215]. Nevertheless, the ESUR MR prostate guidelines recommend that the time interval generally should be at least 3-6 weeks and preliminary T1W imaging should be done to exclude biopsy-related haemorrhage [49]. If significant haemorrhage is present and interferes with examination performance, the patient can then be re-scheduled. However, even though it probably does not alter the final outcome, it is often not feasible in a clinical situation to wait several weeks to months for a staging mp-MRI in a high-risk PCa patient before deciding on the definitive treatment plan.

Conclusion

Mp-MRI prior to repeated biopsies can improve the detection rate of clinically significant PCa and allows for a more accurate GS by combining standard TRUS-bx with mp-MRI-targeted biopsies under visual TRUS-guidance. Mp-MRI can provide valuable information about the histopathological aggressiveness of a PCa lesion and the tumour stage with possible ECE can be assessed in the pre-therapeutic setting providing important additional information for optimal patient-tailored treatment planning.

FUTURE PERSPECTIVES

The role of mp-MRI in our department is rapidly evolving. Clearly, standard TRUS-bx will continue to miss tumours outside the standard biopsy regions and the issue of possible GS undergrading will still be evident. Our gained experience in mp-MRI diagnostics by performing this thesis and studies has now changed our diagnostic approach for patients referred for repeated biopsies. Mp-MRI findings are increasingly relied upon and a diagnostic mp-MRI is performed in all patients with prior negative TRUS-bx and continuous suspicion of PCa. Then additional mp-MRI-bx' of suspicious lesions are performed either in a "targeted-only" approach or added to our standard 10-core TRUS-bx protocol depending on the clinical situation. In study I, we experienced that some PCa lesions were seen on mp-MRI and scored as moderate/high-suspicious regions, but the lesions were missed on the targeted mp-MRI-bx and hit on standard TRUS-bx. We suspect it could be caused by misregistration with visual/cognitive fusion and we are now running a prospective study using software-based mp-MRI/TRUS-fusion biopsies to see if it can increase the accuracy of the mp-MRI-bx, as reported by others comparing the two techniques [126,216,217].

The future impact of PCa patients is predicted to increase rapidly within the next decade. As the post-war "baby boomer" generation continues to age, the incidence of PCa is expected to more than double within the next decades. The positive results of mp-MRI in PCa management have raised the question, whether mp-MRI can be used as a screening test before initial biopsy to increase the detection of aggressive significant PCa while reducing overdetected and possible overtreatment of insignificant PCa foci [125,218]. Several studies of men with no previous biopsies comparing a mp-MRI "targeted-only" approach to a standard TRUS-bx regimen have recently been published [126,135,178,216,219]. A summarised conclusion of these studies shows a promising tendency to decrease the overall detection rate of PCa, but with an increased detection of high-grade cancers using fewer biopsy cores and a decreased detection rate of insignificant tumours. However, mp-MRI is not always cancer-specific and prostate biopsies are still necessary to confirm the presence of PCa in an

abnormal lesion. Nevertheless, the continuous development of the mp-MRI techniques and experience in our department facilitate the future use of mp-MRI as an integrated part in deciding whether or not to perform prostate biopsies at all and where it should be targeted to confirm the diagnosis and hit the most aggressive part of the tumour. It could be the beginning towards the end of blind prostate biopsies [220]. However, mp-MRI-bx may still miss cancer foci and unnecessary targeted biopsies may be conducted due to false-positive mp-MRI readings. The cost-effectiveness of the diagnostic mp-MRI and the additional use of mp-MRI-bx in our department have not yet been calculated. Nonetheless, an image-based mp-MRI-strategy seems to improve patient quality of life by reducing overdiagnosis and overtreatment at comparable costs as the current standard TRUS-bx approach [221].

A major clinical issue in PCa management is accurate risk stratification of newly diagnosed PCa patients and correctly determining if the patient harbours an aggressive cancer that needs active treatment or an insignificant cancer that may be managed by AS. The use of mp-MRI for staging purposes is anticipated to become a more integrated part in the clinical decision-making process at our institution. As mp-MRI has shown promising results in detecting significant PCa missed by TRUS-bx in men diagnosed with low-risk PCa eligible for AS [222–226], patients considered eligible for AS in our institution will increasingly undergo mp-MRI to either confirm the absence of significant PCa or to identify additional suspicious lesions for targeted biopsies. In addition, mp-MRI can be repeated and compared over time as a possible non-invasive alternative to repeated biopsies if necessary. Conversely, newly diagnosed PCa patients with high-risk disease who are considered suitable for RP now undergo a staging mp-MRI at our institution to confirm eligibility for surgery and to provide valuable additional information for optimal surgical planning. Mp-MRI findings can then be combined with clinical findings and nomograms to increase the overall pre-therapeutic diagnostic staging accuracy. However, even though study II showed that mp-MRI with ECE risk scoring evaluated by a dedicated reader is an accurate diagnostic technique in determining tumour stage and ECE at final pathology, further studies are needed to investigate whether functional imaging should be included in the ECE risk scoring scale and if so, how to weigh the individual findings in order to further increase the diagnostic accuracy of the scoring system.

Study III showed that both ADC measurements correlated significantly with the tumour GS at final pathology, but the ADCratio demonstrated the best correlation especially in discriminating $GS \leq 7(3+4)$ from $GS \geq 7(4+3)$ tumours. The next step would be to analyse the ADCratio performance in a true prospective setting by calculating the ADCbenign value prior to surgery without the histopathological map as guidance and with the risk of incorporating small invisible tumour foci. This would be more in line with the workflow in clinical practice. In addition, the inclusion of a second reader to evaluate the inter-observer variation would further explore the diagnostic performance of the ADC measurements.

Lack of experience and standardisation combined with technically unsuitable equipment and lack of functional imaging are reasons why there previously has been a large variation in the prostate MRI readings among different centres. It is evident that mp-MRI interpretation is a specialised task that requires substantial dedication and experience preferably assembled in a centre of excellence. Then, in addition to PCa detection, other specific questions such as exact tumour location, staging, signs of high biological

aggressiveness and possible preservation of NVB at surgery can be addressed in close collaboration between urologists, radiologists, oncologists and pathologists in a multidisciplinary team (MDT) environment to support the clinician's needs. The MDT approach is important, as there are several differential diagnostic conditions in the prostate that may influence the readings as well as the interpretation of the images may be altered depending on the clinical situation to either value high-sensitive or high-specific readings. Furthermore, the interpretation of mp-MRI has a considerable learning curve and education with high-volume readings, conduction of clinical trials comparing results in a close collaboration between radiologists, urologists and pathologists providing feedback to the diagnostic readings based on the clinical and pathological results. A dedicated prostate mp-MRI education program to support mp-MRI readers and technologists interpretatively and technically with certification through reference centres is needed to apply mp-MRI in clinical practice and allow for acceptable diagnostic results.

The constant improvement of mp-MRI and the on-going development of structured MR prostate guidelines will continuously improve the management of PCa patients at our institution. The prostate mp-MRI technique has now been established at our institution, as a first step with the implementation of this PhD project. However, mp-MRI in Denmark is still a new area of research and a new available imaging modality in the clinical practice. The objectives for the future are now to define its specific role in the management of PCa through the continuous development of high-quality acquisitions and readings with clinician-tailored structured reporting in good, fast and simple diagnostic mp-MRI protocols developed for each clinical indication (tumour detection, staging or node and bone) as recommended by the ESUR MR prostate guidelines.

Abbreviations and Acronyms

PSA	Prostate specific antigen
DRE	Digital rectal examination
TRUS	Transrectal ultrasound
TRUS-bx	Transrectal ultrasound guided biopsies
PCa	Prostate cancer
EPE	Extra prostatic tumour extension
RP	Radical prostatectomy
cT	Clinical tumour stage
NVB	Neurovascular bundle
MRI	Magnetic resonance imaging
Mp-MRI	Multiparametric MRI
ESUR	European Society of Urogenital Radiology
PIRADS	Prostate imaging reporting and data system
BIRADS	Breast imaging reporting and data system
T1W	T1-weighted
T2W	T2-weighted
DWI	Diffusion-weighted imaging
ADC	Apparent diffusion coefficient
DCE	Dynamic contrast enhanced
MRSI	Magnetic resonance spectroscopic imaging
GFR	Glomerular filtration rate
OC	Organ-confined
ECE	Extra capsular extension
SVI	Seminal vesicle invasion
GS	Gleason score
ISUP	International Society of Urological Pathology
PZ	Peripheral zone

TZ	Transitional zone
CZ	Central zone
AUC	Area under the curve
MDT	Multi-disciplinary team
BPH	Benign prostate hypertrophy
Re-biopsy	Repeated biopsy
PPA-coil	Pelvic-phased-array coil
ERC	Endo-rectal coil
AS	Active surveillance
PPV	Positive predictive value
NPV	Negative predictive value

SUMMARY

Background:

Prostate cancer (PCa) is the second leading cause of cancer-related mortality and the most frequently diagnosed male malignant disease among men in the Nordic countries. The manifestation of PCa ranges from indolent to highly aggressive disease and due to this high variation in PCa progression, the diagnosis and subsequent treatment planning can be challenging. The current diagnostic approach with PSA testing and digital rectal examination followed by transrectal ultrasound biopsies (TRUS-bx) lack in both sensitivity and specificity in PCa detection and offers limited information about the aggressiveness and stage of the cancer. Scientific work supports the rapidly growing use of multiparametric magnetic resonance imaging (mp-MRI) as the most sensitive and specific imaging tool for detection, lesion characterisation and staging of PCa. However, the experience with mp-MRI in PCa management in Denmark has been very limited. Therefore, we carried out this PhD project based on 3 original studies to evaluate the use of mp-MRI in detection, assessment of biological aggression and staging of PCa in a Danish setup with limited experience in mp-MRI prostate diagnostics. The aim was to assess whether mp-MRI could 1) improve the overall detection rate of clinically significant PCa previously missed by transrectal ultrasound biopsies, 2) identify patients with extracapsular tumour extension and 3) categorize the histopathological aggressiveness based on diffusion-weighted imaging.

Material and methods

Study I included patients with a history of negative TRUS-bx and persistent suspicion of PCa scheduled for repeated biopsies. Mp-MRI was performed prior to the biopsies and analysed for suspicious lesions. All lesions were scored according to the PIRADS classification from the European Society of Urogenital Radiology's (ESUR) MR prostate guidelines. The lesions were given a sum of scores (ranging 3-15) and classified overall on a Likert five-point scale according to the probability of clinically significant malignancy being present. All patients underwent systematic TRUS-bx (10 cores) and visual mp-MRI-targeted biopsies (mp-MRI-bx) under TRUS-guidance of any mp-MRI-suspicious lesion not hit on systematic TRUS-bx.

Study II included patients with clinically localised PCa (cT1-T2) determined by digital rectal examination and/or TRUS and scheduled for radical prostatectomy (RP). Mp-MRI was performed prior to RP and all lesions were evaluated according to the PIRADS classification and the extracapsular extension (ECE) risk scoring from the ESUR MR prostate guidelines. The images were evaluated by two readers with different experience in mp-MRI interpretation. An mp-MRI T-stage (cTMRI) and an ECE risk score were assigned. Additionally, suspicion of ECE was dichotomised into

either organ-confined disease or ECE based on tumour characteristics and personal opinion incorporating functional imaging findings. The RP histopathological results served as standard reference.

Study III included patients from study II, where mean ADC_{tumour} values from all malignant tumour foci ≥ 5 mm identified on histopathology were measured on the corresponding diffusion-weighted imaging ADC_{map}. An ADC_{benign} value was obtained from a non-cancerous area using the histopathological map as a reference to calculate the ADC_{ratio} (ADC_{tumour} divided by ADC_{benign}). The ADC measurements (ADC_{tumour} and ADC_{ratio} values) were correlated with the Gleason score (GS) from each tumour foci.

Results:

Eighty-three patients were included in study I. PCa was found in 39/83 (47%) and both the PIRADS summation score and the overall Likert classification showed a high correlation with biopsy results ($p < 0.0001$). Five patients (13%) had PCa detected only on mp-MRI-bx outside the systematic biopsy areas ($p = 0.025$) and another 7 patients (21%) had an overall GS upgrade of at least one grade ($p = 0.037$) based on the mp-MRI-bx. Clinical significant PCa was found in 37/39 patients according to the Epstein criteria (2004).

Eighty-seven patients were included in study II and underwent mp-MRI before RP. The correlation between cTMRI and pT showed a spearman rho correlation of 0.658 ($p < 0.001$) and 0.306 ($p = 0.004$) with a weighted kappa of 0.585 [CI 0.44;0.73] and 0.22 [CI 0.09;0.35] for reader A and reader B, respectively. The prevalence of ECE after RP was 31/87 (36%). ECE risk scoring showed an AUC of 0.65-0.86 on the ROC-curve for readers and a sensitivity, specificity and diagnostic accuracy of 81% [CI 63;93], 78% [CI 66;88] and 79% at the best cut-off level (risk score ≥ 4) for the most experienced reader. When tumour characteristics were influenced by personal opinion and functional imaging, the sensitivity, specificity and diagnostic accuracy for prediction of ECE changed to 74% [CI 55;88], 88% [CI 76;95] and 83% for reader A and 61% [CI 0.42;0.78], 77% [CI 0.64;0.87] and 71% for reader B, respectively.

Seventy-one patients were included in study III. The association between ADC measurements and GS showed a significantly negative correlation ($p < 0.001$) with spearman rho for ADC_{tumour} (-0.421) and ADC_{ratio} (-0.649), respectively. There was a statistical significant difference between both ADC measurements and the GS groups for all tumours ($p < 0.001$). ROC-curve analysis showed an overall AUC of 0.73 (ADC_{tumour}) to 0.80 (ADC_{ratio}) in discriminating GS 6 from GS ≥ 7 (3+4) tumours. The AUC remained virtually unchanged at 0.72 (ADC_{tumour}), but increased to 0.90 (ADC_{ratio}) when discriminating GS ≤ 7 (3+4) from GS ≥ 7 (4+3).

Conclusion:

Mp-MRI prior to repeated biopsies can improve the detection rate of clinically significant prostate cancer and allow for a more accurate GS by combining standard TRUS-bx with mp-MRI-targeted biopsies under visual TRUS-guidance. Mp-MRI can provide valuable information about the histopathological aggressiveness of a PCa lesion and the tumour stage with possible ECE can be assessed in the pre-therapeutic setting providing important additional information for optimal patient-tailored treatment planning.

REFERENCES

- Engholm G, Ferlay J, Christensen N, Bray F, Gjerstorff ML, Klint A, et al. NORDCAN--a Nordic tool for cancer information, planning, quality control and research. *Acta Oncol* 2010;49:725–36, assessed 06/14, <http://www-dep.iarc.fr/NOR>.
- Heidenreich A, Bastian PJ, Bellmunt J, Bolla M, Joniau S, van der Kwast T, et al. EAU guidelines on prostate cancer. part 1: screening, diagnosis, and local treatment with curative intent-update 2013. *Eur Urol* 2014;65:124–37.
- Hernández J, Thompson IM. Prostate-specific antigen: a review of the validation of the most commonly used cancer biomarker. *Cancer* 2004;101:894–904.
- Thompson IM, Pauler DK, Goodman PJ, Tangen CM, Lucia MS, Parnes HL, et al. Prevalence of prostate cancer among men with a prostate-specific antigen level < or =4.0 ng per milliliter. *N Engl J Med* 2004;350:2239–46.
- Catalona WJ, Hudson MA, Scardino PT, Richie JP, Ahmann FR, Flanigan RC, et al. Selection of optimal prostate specific antigen cutoffs for early detection of prostate cancer: receiver operating characteristic curves. *J Urol* 1994;152:2037–42.
- De Angelis G, Rittenhouse HG, Mikolajczyk SD, Blair Shamel L, Semjonow A. Twenty Years of PSA: From Prostate Antigen to Tumor Marker. *Rev Urol* 2007;9:113–23.
- Djavan B, Ravery V, Zlotta A, Dobronski P, Dobrovits M, Fakhari M, et al. Prospective evaluation of prostate cancer detected on biopsies 1, 2, 3 and 4: when should we stop? *J Urol* 2001;166:1679–83.
- Obort AS, Ajadi MB, Akinloye O. Prostate-specific antigen: any successor in sight? *Rev Urol* 2013;15:97–107.
- Carvalho GF, Smith DS, Mager DE, Ramos C, Catalona WJ. Digital rectal examination for detecting prostate cancer at prostate specific antigen levels of 4 ng./ml. or less. *J Urol* 1999;161:835–9.
- Varenhorst E, Berglund K, Löfman O, Pedersen K. Inter-observer variation in assessment of the prostate by digital rectal examination. *Br J Urol* 1993;72:173–6.
- Chodak GW. Early detection and screening for prostatic cancer. *Urology* 1989;34:10–2; discussion 46–56.
- Pedersen K V, Carlsson P, Varenhorst E, Löfman O, Berglund K. Screening for carcinoma of the prostate by digital rectal examination in a randomly selected population. *BMJ* 1990;300:1041–4.
- Catalona WJ, Richie JP, Ahmann FR, Hudson MA, Scardino PT, Flanigan RC, et al. Comparison of digital rectal examination and serum prostate specific antigen in the early detection of prostate cancer: results of a multicenter clinical trial of 6,630 men. *J Urol* 1994;151:1283–90.
- Gosselaar C, Roobol MJ, Roemeling S, Schröder FH. The role of the digital rectal examination in subsequent screening visits in the European randomized study of screening for prostate cancer (ERSPC), Rotterdam. *Eur Urol* 2008;54:581–8.
- Okotie OT, Roehl KA, Han M, Loeb S, Gashti SN, Catalona WJ. Characteristics of prostate cancer detected by digital rectal examination only. *Urology* 2007;70:1117–20.
- Heidenreich A, Bolla M, Joniau S, Kwast TH Van Der, Matveev V, Mason MD, et al. Guidelines on Prostate Cancer 2009.
- Harvey CJ, Pilcher J, Richenberg J, Patel U, Frauscher F. Applications of transrectal ultrasound in prostate cancer. *Br J Radiol* 2012;85 Spec No:S3–17.
- Spajic B, Eupic H, Tomas D, Stimac G, Kruslin B, Kraus O. The incidence of hyperechoic prostate cancer in transrectal ultrasound-guided biopsy specimens. *Urology* 2007;70:734–7.
- Ukimura O, Coleman JA, de la Taille A, Emberton M, Epstein JI, Freedland SJ, et al. Contemporary role of systematic prostate biopsies: indications, techniques, and implications for patient care. *Eur Urol* 2013;63:214–30.
- Shariat SF, Roehrborn CG. Using biopsy to detect prostate cancer. *Rev Urol* 2008;10:262–80.
- Serefoglu EC, Altinova S, Ugras NS, Akincioglu E, Asil E, Balbay MD. How reliable is 12-core prostate biopsy procedure in the detection of prostate cancer? *Can Urol Assoc J* 2012;1–6.
- Roehrborn CG, Pickens GJ, Sanders JS. Diagnostic yield of repeated transrectal ultrasound-guided biopsies stratified by specific histopathologic diagnoses and prostate specific antigen levels. *Urology* 1996;47:347–52.
- Ploussard G, Nicolaiew N, Marchand C, Terry S, Vacherot F, Vordos D, et al. Prospective Evaluation of an Extended 21-Core Biopsy Scheme as Initial Prostate Cancer Diagnostic Strategy. *Eur Urol* 2012.
- Maccagnano C, Gallina A, Roscigno M, Raber M, Capitanio U, Saccà A, et al. Prostate saturation biopsy following a first negative biopsy: state of the art. *Urol Int* 2012;89:126–35.
- Zaytoun OM, Moussa AS, Gao T, Fareed K, Jones JS. Office based transrectal saturation biopsy improves prostate cancer detection compared to extended biopsy in the repeat biopsy population. *J Urol* 2011;186:850–4.
- Boccon-Gibod LM, Dumonceau O, Toubianc M, Ravery V, Boccon-Gibod LA. Micro-focal prostate cancer: a comparison of biopsy and radical prostatectomy specimen features. *Eur Urol* 2005;48:895–9.
- Epstein JI, Allsbrook WC, Amin MB, Egevad LL. The 2005 International Society of Urological Pathology (ISUP) Consensus Conference on Gleason Grading of Prostatic Carcinoma. *Am J Surg Pathol* 2005;29:1228–42.
- Gleason DF, Mellinger GT. Prediction of prognosis for prostatic adenocarcinoma by combined histological grading and clinical staging. *J Urol* 1974;111:58–64.
- Epstein JI, Allsbrook WC, Amin MB, Egevad LL. Update on the Gleason Grading System for Prostate Cancer Urologic Pathologists 2006;13:57–9.
- Egevad L, Granfors T, Karlberg L, Bergh A, Stattin P. Prognostic value of the Gleason score in prostate cancer. *BJU Int* 2002;89:538–42.
- Rusthoven CG, Carlson JA, Waxweiler T V, Yeh N, Raben D, Flaig TW, et al. The prognostic significance of Gleason scores in metastatic prostate cancer. *Urol Oncol* 2014;32:707–13.
- Brimo F, Montironi R, Egevad L, Erbersdobler A, Lin DW, Nelson JB, et al. Contemporary grading for prostate cancer: implications for patient care. *Eur Urol* 2013;63:892–901.
- Pierorazio PM, Walsh PC, Partin AW, Epstein JI. Prognostic Gleason grade grouping: data based on the modified Gleason scoring system. *BJU Int* 2013;111:753–60.
- Epstein JI, Feng Z, Trock BJ, Pierorazio PM. Upgrading and downgrading of prostate cancer from biopsy to radical prostatectomy: incidence and predictive factors using the

- modified Gleason grading system and factoring in tertiary grades. *Eur Urol* 2012;61:1019–24.
35. Delahunt B, Miller RJ, Srigley JR, Evans AJ, Samaratunga H. Gleason grading: past, present and future. *Histopathology* 2012;60:75–86.
 36. Sobin L, Gospodarowicz M WC. *TNM Classification of Malignant Tumours . Urological Tumours*. Seventh edition, International Union Against Cancer. 7 th. Hoboken, NJ: Wiley-Blackwell; 2009.
 37. Mullerad M, Hricak H, Kuroiwa K, Pucar D, Chen H-N, Kattan MW, et al. Comparison of endorectal magnetic resonance imaging, guided prostate biopsy and digital rectal examination in the preoperative anatomical localization of prostate cancer. *J Urol* 2005;174:2158–63.
 38. Grossfeld GD, Chang JJ, Broering JM, Li YP, Lubeck DP, Flanders SC, et al. Under staging and under grading in a contemporary series of patients undergoing radical prostatectomy: results from the Cancer of the Prostate Strategic Urologic Research Endeavor database. *J Urol* 2001;165:851–6.
 39. Partin AW, Carter HB, Chan DW, Epstein JI, Oesterling JE, Rock RC, et al. Prostate specific antigen in the staging of localized prostate cancer: influence of tumor differentiation, tumor volume and benign hyperplasia. *J Urol* 1990;143:747–52.
 40. Lange PH, Ercole CJ, Lightner DJ, Fraley EE, Vessella R. The value of serum prostate specific antigen determinations before and after radical prostatectomy. *J Urol* 1989;141:873–9.
 41. Hudson MA, Bahnson RR, Catalona WJ. Clinical use of prostate specific antigen in patients with prostate cancer. *J Urol* 1989;142:1011–7.
 42. D'Amico A V, Whittington R, Malkowicz SB, Schultz D, Blank K, Broderick GA, et al. Biochemical outcome after radical prostatectomy, external beam radiation therapy, or interstitial radiation therapy for clinically localized prostate cancer. *JAMA* 1998;280:969–74.
 43. D'Amico A V, Whittington R, Malkowicz SB, Cote K, Loffredo M, Schultz D, et al. Biochemical outcome after radical prostatectomy or external beam radiation therapy for patients with clinically localized prostate carcinoma in the prostate specific antigen era. *Cancer* 2002;95:281–6.
 44. Wang L, Hricak H, Kattan MW, Chen H-N, Scardino PT, Kuroiwa K. Prediction of organ-confined prostate cancer: incremental value of MR imaging and MR spectroscopic imaging to staging nomograms. *Radiology* 2006;238:597–603.
 45. Otori M, Kattan MW, Koh H, Maru N, Slawin KM, Shariat S, et al. Predicting the presence and side of extracapsular extension: a nomogram for staging prostate cancer. *J Urol* 2004;171:1844–9; discussion 1849.
 46. Eifler JB, Feng Z, Lin BM, Partin MT, Humphreys EB, Han M, et al. An updated prostate cancer staging nomogram (Partin tables) based on cases from 2006 to 2011. *BJU Int* 2013;111:22–9.
 47. Steyn JH, Smith FW. Nuclear magnetic resonance imaging of the prostate. *Br J Urol* 1982;54:726–8.
 48. Sciarra A, Barentsz J, Bjartell A, Eastham J, Hricak H, Panebianco V, et al. Advances in magnetic resonance imaging: how they are changing the management of prostate cancer. *Eur Urol* 2011;59:962–77.
 49. Borre M, Lundorf E, Marcussen N, Langkilde NC, Wolf H. Phased array magnetic resonance imaging for staging clinically localised prostate cancer. *Acta Oncol* 2005;44:589–92.
 50. Chabanova E, Balslev I, Logager V, Hansen A, Jakobsen H, Kromann-Andersen B, et al. Prostate cancer: 1.5 T endo-coil dynamic contrast-enhanced MRI and MR spectroscopy--correlation with prostate biopsy and prostatectomy histopathological data. *Eur J Radiol* 2011;80:292–6.
 51. Barentsz JO, Richenberg J, Clements R, Choyke P, Verma S, Villeirs G, et al. ESUR prostate MR guidelines 2012. *Eur Radiol* 2012;22:746–57.
 52. Heijmink SWTPJ, Fütterer JJ, Hambrock T, Takahashi S, Scheenen TWJ, Huisman HJ, et al. Prostate cancer: body-array versus endorectal coil MR imaging at 3 T--comparison of image quality, localization, and staging performance. *Radiology* 2007;244:184–95.
 53. Turkbey B, Merino MJ, Gallardo EC, Shah V, Aras O, Bernardo M, et al. Comparison of endorectal coil and nonendorectal coil T2W and diffusion-weighted MRI at 3 Tesla for localizing prostate cancer: correlation with whole-mount histopathology. *J Magn Reson Imaging* 2014;39:1443–8.
 54. Heijmink SWTPJ, Fütterer JJ, Strum SS, Oyen WJG, Frauscher F, Witjes JA, et al. State-of-the-art urologic imaging in the diagnosis of prostate cancer. *Acta Oncol* 2011;50 Suppl 1:25–38.
 55. Boesen L, Thomsen HS. Magnetic resonance imaging in management of prostate cancer.. *Ugeskr Laeger* 2013;175:1630–3.
 56. Boesen L, Thomsen HS. Magnetic resonance imaging facilitate appropriate treatment selection of prostate cancer patients.. *Ugeskr Laeger* 2013;175:1634–7.
 57. Hambrock T, Hoeks C, Hulsbergen-van de Kaa C, Scheenen T, Fütterer J, Bouwense S, et al. Prospective assessment of prostate cancer aggressiveness using 3-T diffusion-weighted magnetic resonance imaging-guided biopsies versus a systematic 10-core transrectal ultrasound prostate biopsy cohort. *Eur Urol* 2012;61:177–84.
 58. Turkbey B, Shah VP, Pang Y, Bernardo M, Xu S, Kruecker J, et al. Is apparent diffusion coefficient associated with clinical risk scores for prostate cancers that are visible on 3-T MR images? *Radiology* 2011;258:488–95.
 59. Kumar R, Nayyar R, Kumar V, Gupta NP, Hemal AK, Jagannathan NR, et al. Potential of magnetic resonance spectroscopic imaging in predicting absence of prostate cancer in men with serum prostate-specific antigen between 4 and 10 ng/ml: a follow-up study. *Urology* 2008;72:859–63.
 60. Villeirs GM, De Meerleer GO, De Visschere PJ, Fonteyne VH, Verbaeys AC, Oosterlinck W. Combined magnetic resonance imaging and spectroscopy in the assessment of high grade prostate carcinoma in patients with elevated PSA: a single-institution experience of 356 patients. *Eur J Radiol* 2011;77:340–5.
 61. Tamada T, Sone T, Jo Y, Yamamoto A, Yamashita T, Egashira N, et al. Prostate cancer: relationships between postbiopsy hemorrhage and tumor detectability at MR diagnosis. *Radiology* 2008;248:531–9.
 62. White S, Hricak H, Forstner R, Kurhanewicz J, Vigneron DB, Zaloudek CJ, et al. Prostate cancer: effect of postbiopsy hemorrhage on interpretation of MR images. *Radiology* 1995;195:385–90.
 63. Barrett T, Vargas HA, Akin O, Goldman DA, Hricak H. Value of the hemorrhage exclusion sign on T1-weighted prostate

- MR images for the detection of prostate cancer. *Radiology* 2012;263:751–7.
64. Vargas HA, Akin O, Franiel T, Goldman DA, Udo K, Touijer KA, et al. Normal central zone of the prostate and central zone involvement by prostate cancer: clinical and MR imaging implications. *Radiology* 2012;262:894–902.
 65. Cruz M, Tsuda K, Narumi Y, Kuroiwa Y, Nose T, Kojima Y, et al. Characterization of low-intensity lesions in the peripheral zone of prostate on pre-biopsy endorectal coil MR imaging. *Eur Radiol* 2002;12:357–65.
 66. Turkbey B, Albert PS, Kurdziel K, Choyke PL. Imaging localized prostate cancer: current approaches and new developments. *AJR Am J Roentgenol* 2009;192:1471–80.
 67. Akin O, Sala E, Moskowitz CS, Kuroiwa K, Ishill NM, Pucar D, et al. Transition zone prostate cancers: features, detection, localization, and staging at endorectal MR imaging. *Radiology* 2006;239:784–92.
 68. Wang L, Mazaheri Y, Zhang J, Ishill NM, Kuroiwa K, Hricak H. Assessment of biologic aggressiveness of prostate cancer: correlation of MR signal intensity with Gleason grade after radical prostatectomy. *Radiology* 2008;246:168–76.
 69. Langer DL, van der Kwast TH, Evans AJ, Sun L, Yaffe MJ, Trachtenberg J, et al. Intermixed normal tissue within prostate cancer: effect on MR imaging measurements of apparent diffusion coefficient and T2--sparse versus dense cancers. *Radiology* 2008;249:900–8.
 70. Tan CH, Wei W, Johnson V, Kundra V. Diffusion-weighted MRI in the detection of prostate cancer: meta-analysis. *AJR Am J Roentgenol* 2012;199:822–9.
 71. Fuchsjäger M, Shukla-Dave a, Akin O, Barentsz J, Hricak H. Prostate cancer imaging. *Acta Radiol* 2008;49:107–20.
 72. Cornud F, Rouanne M, Beuvon F, Eiss D, Flam T, Liberatore M, et al. Endorectal 3D T2-weighted 1mm-slice thickness MRI for prostate cancer staging at 1.5Tesla: should we reconsider the indirect signs of extracapsular extension according to the D'Amico tumor risk criteria? *Eur J Radiol* 2012;81:591–7.
 73. Verma S, Rajesh A. A clinically relevant approach to imaging prostate cancer: review. *AJR Am J Roentgenol* 2011;196:S1–10.
 74. Sala E, Akin O, Moskowitz CS, Eisenberg HF, Kuroiwa K, Ishill NM, et al. Endorectal MR imaging in the evaluation of seminal vesicle invasion: diagnostic accuracy and multivariate feature analysis. *Radiology* 2006;238:929–37.
 75. Qayyum A. Diffusion-weighted imaging in the abdomen and pelvis: concepts and applications. *Radiographics* 2009;29:1797–810.
 76. Kim CK, Park BK, Kim B. Diffusion-weighted MRI at 3 T for the evaluation of prostate cancer. *AJR Am J Roentgenol* 2010;194:1461–9.
 77. Somford DM, Fütterer JJ, Hambrock T, Barentsz JO. Diffusion and perfusion MR imaging of the prostate. *Magn Reson Imaging Clin N Am* 2008;16:685–95.
 78. Zelhof B, Pickles M, Liney G, Gibbs P, Rodrigues G, Kraus S, et al. Correlation of diffusion-weighted magnetic resonance data with cellularity in prostate cancer. *BJU Int* 2009;103:883–8.
 79. Gibbs P, Pickles MD, Turnbull LW. Diffusion imaging of the prostate at 3.0 tesla. *Invest Radiol* 2006;41:185–8.
 80. Wu L-M, Xu J-R, Ye Y-Q, Lu Q, Hu J-N. The clinical value of diffusion-weighted imaging in combination with T2-weighted imaging in diagnosing prostate carcinoma: a systematic review and meta-analysis. *AJR Am J Roentgenol* 2012;199:103–10.
 81. Verma S, Rajesh A, Morales H, Lemen L, Bills G, Delworth M, et al. Assessment of aggressiveness of prostate cancer: correlation of apparent diffusion coefficient with histologic grade after radical prostatectomy. *AJR Am J Roentgenol* 2011;196:374–81.
 82. Hambrock T, Somford DM, Huisman HJ, van Oort IM, Witjes JA, Hulsbergen-van de Kaa CA, et al. Relationship between apparent diffusion coefficients at 3.0-T MR imaging and Gleason grade in peripheral zone prostate cancer. *Radiology* 2011;259:453–61.
 83. Vargas HA, Akin O, Franiel T, Mazaheri Y, Zheng J, Moskowitz C, et al. Diffusion-weighted endorectal MR imaging at 3 T for prostate cancer: tumor detection and assessment of aggressiveness. *Radiology* 2011;259:775–84.
 84. Jung S II, Donati OF, Vargas HA, Goldman D, Hricak H, Akin O. Transition zone prostate cancer: incremental value of diffusion-weighted endorectal MR imaging in tumor detection and assessment of aggressiveness. *Radiology* 2013;269:493–503.
 85. Van As NJ, de Souza NM, Riches SF, Morgan VA, Sohaib SA, Dearnaley DP, et al. A study of diffusion-weighted magnetic resonance imaging in men with untreated localised prostate cancer on active surveillance. *Eur Urol* 2009;56:981–7.
 86. Thörmer G, Otto J, Reiss-Zimmermann M, Seiwerts M, Moche M, Garnov N, et al. Diagnostic value of ADC in patients with prostate cancer: influence of the choice of b values. *Eur Radiol* 2012;22:1820–8.
 87. Litjens GJS, Hambrock T, Hulsbergen-van de Kaa C, Barentsz JO, Huisman HJ. Interpatient variation in normal peripheral zone apparent diffusion coefficient: effect on the prediction of prostate cancer aggressiveness. *Radiology* 2012;265:260–6.
 88. Oto A, Kayhan A, Jiang Y, Tretiakova M, Yang C, Antic T, et al. Prostate cancer: differentiation of central gland cancer from benign prostatic hyperplasia by using diffusion-weighted and dynamic contrast-enhanced MR imaging. *Radiology* 2010;257:715–23.
 89. Litjens GJS, Hambrock T, Hulsbergen-van de Kaa C, Barentsz JO, Huisman HJ. Interpatient variation in normal peripheral zone apparent diffusion coefficient: effect on the prediction of prostate cancer aggressiveness. *Radiology* 2012;265:260–6.
 90. Kim JH, Kim JK, Park B-W, Kim N, Cho K-S. Apparent diffusion coefficient: prostate cancer versus noncancerous tissue according to anatomical region. *J Magn Reson Imaging* 2008;28:1173–9.
 91. Tamada T, Sone T, Jo Y, Toshimitsu S, Yamashita T, Yamamoto A, et al. Apparent diffusion coefficient values in peripheral and transition zones of the prostate: comparison between normal and malignant prostatic tissues and correlation with histologic grade. *J Magn Reson Imaging* 2008;28:720–6.
 92. Alonzi R, Padhani AR, Allen C. Dynamic contrast enhanced MRI in prostate cancer. *Eur J Radiol* 2007;63:335–50.
 93. Brawer MK, Deering RE, Brown M, Preston SD, Bigler SA. Predictors of pathologic stage in prostatic carcinoma. The role of neovascularity. *Cancer* 1994;73:678–87.
 94. Bigler SA, Deering RE, Brawer MK. Comparison of microscopic vascularity in benign and malignant prostate tissue. *Hum Pathol* 1993;24:220–6.

95. Noworolski SM, Henry RG, Vigneron DB, Kurhanewicz J. Dynamic contrast-enhanced MRI in normal and abnormal prostate tissues as defined by biopsy, MRI, and 3D MRSI. *Magn Reson Med* 2005;53:249–55.
96. Choi YJ, Kim JK, Kim N, Kim KW, Choi EK, Cho K-S. Functional MR imaging of prostate cancer. *Radiographics* 2007;27:63–75.
97. Verma S, Turkbey B, Muradyan N, Rajesh A, Cornud F, Haider MA, et al. Overview of dynamic contrast-enhanced MRI in prostate cancer diagnosis and management. *AJR Am J Roentgenol* 2012;198:1277–88.
98. Ocak I, Bernardo M, Metzger G, Barrett T, Pinto P, Albert PS, et al. Dynamic contrast-enhanced MRI of prostate cancer at 3 T: a study of pharmacokinetic parameters. *AJR Am J Roentgenol* 2007;189:849.
99. Hara N, Okuizumi M, Koike H, Kawaguchi M, Bilim V. Dynamic contrast-enhanced magnetic resonance imaging (DCE-MRI) is a useful modality for the precise detection and staging of early prostate cancer. *Prostate* 2005;62:140–7.
100. Turkbey B, Pinto PA, Mani H, Bernardo M, Pang Y, McKinney YL, et al. Prostate cancer: value of multiparametric MR imaging at 3 T for detection--histopathologic correlation. *Radiology* 2010;255:89–99.
101. Fütterer JJ, Heijmink SWTPJ, Scheenen TWJ, Veltman J, Huisman HJ, Vos P, et al. Prostate cancer localization with dynamic contrast-enhanced MR imaging and proton MR spectroscopic imaging. *Radiology* 2006;241:449–58.
102. Bloch BN, Furman-Haran E, Helbich TH, Lenkinski RE, Degani H, Kratzik C, et al. Prostate cancer: accurate determination of extracapsular extension with high-spatial-resolution dynamic contrast-enhanced and T2-weighted MR imaging--initial results. *Radiology* 2007;245:176–85.
103. Cirillo S, Petracchini M, Scotti L, Gallo T, Macera A, Bona MC, et al. Endorectal magnetic resonance imaging at 1.5 Tesla to assess local recurrence following radical prostatectomy using T2-weighted and contrast-enhanced imaging. *Eur Radiol* 2009;19:761–9.
104. Haider MA, Chung P, Sweet J, Toi A, Jhaveri K, Ménard C, et al. Dynamic contrast-enhanced magnetic resonance imaging for localization of recurrent prostate cancer after external beam radiotherapy. *Int J Radiat Oncol Biol Phys* 2008;70:425–30.
105. Yakar D, Hambrock T, Huisman H, Hulsbergen-van de Kaa C a, van Lin E, Vergunst H, et al. Feasibility of 3T dynamic contrast-enhanced magnetic resonance-guided biopsy in localizing local recurrence of prostate cancer after external beam radiation therapy. *Invest Radiol* 2010;45:121–5.
106. Wu LM, Xu J-R, Gu HY, Hua J, Zhu J, Chen J, et al. Role of magnetic resonance imaging in the detection of local prostate cancer recurrence after external beam radiotherapy and radical prostatectomy. *Clin Oncol (R Coll Radiol)* 2013;25:252–64.
107. Panebianco V, Barchetti F, Sciarra A, Musio D, Forte V, Gentile V, et al. Prostate cancer recurrence after radical prostatectomy: the role of 3-T diffusion imaging in multiparametric magnetic resonance imaging. *Eur Radiol* 2013;23:1745–52.
108. Baur ADJ, Maxeiner A, Franiel T, Kilic E, Huppertz A, Schwenke C, et al. Evaluation of the prostate imaging reporting and data system for the detection of prostate cancer by the results of targeted biopsy of the prostate. *Invest Radiol* 2014;49:411–20.
109. Engelbrecht MR, Huisman HJ, Laheij RJF, Jager GJ, van Leenders GJLH, Hulsbergen-Van De Kaa CA, et al. Discrimination of prostate cancer from normal peripheral zone and central gland tissue by using dynamic contrast-enhanced MR imaging. *Radiology* 2003;229:248–54.
110. Mullerad M, Hricak H, Wang L, Chen H-N, Kattan MW, Scardino PT. Prostate cancer: detection of extracapsular extension by genitourinary and general body radiologists at MR imaging. *Radiology* 2004;232:140–6.
111. Fütterer JJ, Engelbrecht MR, Huisman HJ, Jager GJ, Hulsbergen-van De Kaa CA, Witjes JA, et al. Staging prostate cancer with dynamic contrast-enhanced endorectal MR imaging prior to radical prostatectomy: experienced versus less experienced readers. *Radiology* 2005;237:541–9.
112. Wassberg C, Akin O, Vargas HA, Shukla-Dave A, Zhang J, Hricak H. The incremental value of contrast-enhanced MRI in the detection of biopsy-proven local recurrence of prostate cancer after radical prostatectomy: effect of reader experience. *AJR Am J Roentgenol* 2012;199:360–6.
113. Engelbrecht MR, Jager GJ, Laheij RJ, Verbeek ALM, van Lier HJ, Barentsz JO. Local staging of prostate cancer using magnetic resonance imaging: a meta-analysis. *Eur Radiol* 2002;12:2294–302.
114. Fütterer JJ, Engelbrecht MR, Jager GJ, Hartman RP, King BF, Hulsbergen-Van de Kaa CA, et al. Prostate cancer: comparison of local staging accuracy of pelvic phased-array coil alone versus integrated endorectal-pelvic phased-array coils. Local staging accuracy of prostate cancer using endorectal coil MR imaging. *Eur Radiol* 2007;17:1055–65.
115. Hoeks CMA, Barentsz JO, Hambrock T, Yakar D, Somford DM, Heijmink SWTPJ, et al. Prostate cancer: multiparametric MR imaging for detection, localization, and staging. *Radiology* 2011;261:46–66.
116. Brajtborde JS, Lavery HJ, Nabizada-Pace F, Senaratne P, Samadi DB. Endorectal magnetic resonance imaging has limited clinical ability to preoperatively predict pT3 prostate cancer. *BJU Int* 2011;107:1419–24.
117. Heidenreich A. Consensus criteria for the use of magnetic resonance imaging in the diagnosis and staging of prostate cancer: not ready for routine use. *Eur Urol* 2011;59:495–7.
118. Roethke MC, Kuru TH, Schultze S, Tichy D, Kopp-Schneider A, Fenchel M, et al. Evaluation of the ESUR PI-RADS scoring system for multiparametric MRI of the prostate with targeted MR/TRUS fusion-guided biopsy at 3.0 Tesla. *Eur Radiol* 2014;24:344–52.
119. Bomers JGR, Barentsz JO. Standardization of Multiparametric Prostate MR Imaging Using PI-RADS. *Biomed Res Int* 2014;doi:10.1155/2014/431680.
120. Rosenkrantz AB, Chandarana H, Gilet A, Deng F-M, Babb JS, Melamed J, et al. Prostate cancer: utility of diffusion-weighted imaging as a marker of side-specific risk of extracapsular extension. *J Magn Reson Imaging* 2013;38:312–9.
121. Chong Y, Kim CK, Park SY, Park BK, Kwon GY, Park JJ. Value of diffusion-weighted imaging at 3 T for prediction of extracapsular extension in patients with prostate cancer: a preliminary study. *AJR Am J Roentgenol* 2014;202:772–7.
122. Gupta RT, Kauffman CR, Polascik TJ, Taneja SS, Rosenkrantz AB. The state of prostate MRI in 2013. *Oncology* 2013;27:262–70.
123. Penzkofer T, Tempny-Afdhal CM. Prostate cancer detection and diagnosis: the role of MR and its comparison

- with other diagnostic modalities - a radiologist's perspective. *NMR Biomed* 2014;27:3–15.
124. Thompson J, Lawrentschuk N, Frydenberg M, Thompson L, Stricker P. The role of magnetic resonance imaging in the diagnosis and management of prostate cancer. *BJU Int* 2013;112 Suppl:6–20.
 125. Barentsz JO, Heijmink SWTPJ, Kaa CH Der, Hoeks C, Futterer JJ. Magnetic Resonance Imaging of Prostate Cancer. *Dis. Abdomen Pelvis* 2010-2013, Springer; 2013, p. 125–42.
 126. Johnson LM, Turkbey B, Figg WD, Choyke PL. Multiparametric MRI in prostate cancer management. *Nat Rev Clin Oncol* 2014;11:346–53.
 127. Cornud F, Delongchamps NB, Mozer P, Beuvon F, Schull a, Muradyan N, et al. Value of multiparametric MRI in the work-up of prostate cancer. *Curr Urol Rep* 2012;13:82–92.
 128. Moore CM, Robertson NL, Arsanious N, Middleton T, Villers A, Klotz L, et al. Image-guided prostate biopsy using magnetic resonance imaging-derived targets: a systematic review. *Eur Urol* 2013;63:125–40.
 129. Delongchamps NB, Peyromaure M, Schull A, Beuvon F, Bouazza N, Flam T, et al. Prebiopsy magnetic resonance imaging and prostate cancer detection: comparison of random and targeted biopsies. *J Urol* 2013;189:493–9.
 130. Lawrentschuk N, Fleshner N. The role of magnetic resonance imaging in targeting prostate cancer in patients with previous negative biopsies and elevated prostate-specific antigen levels. *BJU Int* 2009;103:730–3.
 131. Hoeks CM a, Schouten MG, Bomers JGR, Hoogendoorn SP, Hulsbergen-van de Kaa C a, Hambrock T, et al. Three-Tesla magnetic resonance-guided prostate biopsy in men with increased prostate-specific antigen and repeated, negative, random, systematic, transrectal ultrasound biopsies: detection of clinically significant prostate cancers. *Eur Urol* 2012;62:902–9.
 132. Habchi H, Bratan F, Paye A, Pagnoux G, Sanzalone T, Mège-Lechevallier F, et al. Value of prostate multiparametric magnetic resonance imaging for predicting biopsy results in first or repeat biopsy. *Clin Radiol* 2014;69:120–8.
 133. Portalez D, Rollin G, Leandri P, Elman B, Mouly P, Jonca F, et al. Prospective comparison of T2w-MRI and dynamic-contrast-enhanced MRI, 3D-MR spectroscopic imaging or diffusion-weighted MRI in repeat TRUS-guided biopsies. *Eur Radiol* 2010;20:2781–90.
 134. Labanaris AP, Engelhard K, Zugor V, Nützel R, Kühn R. Prostate cancer detection using an extended prostate biopsy schema in combination with additional targeted cores from suspicious images in conventional and functional endorectal magnetic resonance imaging of the prostate. *Prostate Cancer Prostatic Dis* 2010;13:65–70.
 135. Siddiqui MM, Rais-Bahrami S, Truong H, Stamatakis L, Vourganti S, Nix J, et al. Magnetic Resonance Imaging/Ultrasound-Fusion Biopsy Significantly Upgrades Prostate Cancer Versus Systematic 12-core Transrectal Ultrasound Biopsy. *Eur Urol* 2013;64:713–9.
 136. Dickinson L, Ahmed HU, Allen C, Barentsz JO, Carey B, Futterer JJ, et al. Magnetic resonance imaging for the detection, localisation, and characterisation of prostate cancer: recommendations from a European consensus meeting. *Eur Urol* 2011;59:477–94.
 137. Barentsz J, Villers A, Schouten M. ESUR prostate MR guidelines. Author reply. *Eur Radiol* 2013;23:2322–3.
 138. Haffner J, Lemaitre L, Puech P, Haber G-P, Leroy X, Jones JS, et al. Role of magnetic resonance imaging before initial biopsy: comparison of magnetic resonance imaging-targeted and systematic biopsy for significant prostate cancer detection. *BJU Int* 2011;108:E171–8.
 139. Soulié M. What is the Role of Surgery for Locally Advanced Disease? *Eur Urol Suppl* 2008;7:400–5.
 140. Hegde J V, Chen M-H, Mulkern R V, Fennessy FM, D'Amico A V, Tempany CMC. Preoperative 3-Tesla multiparametric endorectal magnetic resonance imaging findings and the odds of upgrading and upstaging at radical prostatectomy in men with clinically localized prostate cancer. *Int J Radiat Oncol Biol Phys* 2013;85:101–7.
 141. Renard-Penna R, Rouprêt M, Comperat E, Ayed A, Coudert M, Mozer P, et al. Accuracy of high resolution (1.5 tesla) pelvic phased array magnetic resonance imaging (MRI) in staging prostate cancer in candidates for radical prostatectomy: results from a prospective study. *Urol Oncol* 2013;31:448–54.
 142. Portalez D, Mozer P, Cornud F, Renard-Penna R, Misrai V, Thoulouzan M, et al. Validation of the European Society of Urogenital Radiology scoring system for prostate cancer diagnosis on multiparametric magnetic resonance imaging in a cohort of repeat biopsy patients. *Eur Urol* 2012;62:986–96.
 143. Röthke M, Blondin D, Schlemmer H-P, Franiel T. PI-RADS classification: structured reporting for MRI of the prostate.. *Rofo* 2013;185:253–61.
 144. Boesen L, Noergaard N, Chabanova E, Logager V, Balslev I, Mikines K, et al. Early experience with multiparametric magnetic resonance imaging-targeted biopsies under visual transrectal ultrasound guidance in patients suspicious for prostate cancer undergoing repeated biopsy. *Scand J Urol* 2014:Epub ahead of print., doi:10.3109/21681805.2014.9.
 145. Rosenkrantz AB, Kim S, Lim RP, Hindman N, Deng F-M, Babb JS, et al. Prostate cancer localization using multiparametric MR imaging: comparison of Prostate Imaging Reporting and Data System (PI-RADS) and Likert scales. *Radiology* 2013;269:482–92.
 146. Ching CB, Moussa AS, Li J, Lane BR, Zippe C, Jones JS. Does transrectal ultrasound probe configuration really matter? End fire versus side fire probe prostate cancer detection rates. *J Urol* 2009;181:2077–82; discussion 2082–3.
 147. Hoeks CMA, Hambrock T, Yakar D, Hulsbergen-van de Kaa CA, Feuth T, Witjes JA, et al. Transition zone prostate cancer: detection and localization with 3-T multiparametric MR imaging. *Radiology* 2013;266:207–17.
 148. Lemaitre L, Puech P, Poncelet E, Bouyé S, Leroy X, Biserte J, et al. Dynamic contrast-enhanced MRI of anterior prostate cancer: morphometric assessment and correlation with radical prostatectomy findings. *Eur Radiol* 2009;19:470–80.
 149. Ouzzane A, Puech P, Lemaitre L, Leroy X, Nevoux P, Betrouni N, et al. Combined multiparametric MRI and targeted biopsies improve anterior prostate cancer detection, staging, and grading. *Urology* 2011;78:1356–62.
 150. Ploussard G, Aronson S, Pelsers V, Levental M, Anidjar M, Bladou F. Impact of the type of ultrasound probe on prostate cancer detection rate and characterization in patients undergoing MRI-targeted prostate biopsies using cognitive fusion. *World J Urol* 2013;32(4):977–83.
 151. Pinto PA, Chung PH, Rastinehad AR, Baccala AA, Kruecker J, Benjamin CJ, et al. Magnetic resonance imaging/ultrasound fusion guided prostate biopsy improves cancer detection following transrectal ultrasound biopsy and correlates with

- multiparametric magnetic resonance imaging. *J Urol* 2011;186:1281–5.
152. Volkin D, Turkbey B, Hoang AN, Rais-Bahrami S, Yerram N, Walton-Diaz A, et al. Multiparametric MRI and Subsequent MR/Ultrasound Fusion-Guided Biopsy Increase the Detection of Anteriorly Located Prostate Cancers. *BJU Int* 2014:Epub ahead of print., doi:10.1111/bju.12670.
 153. Mozer P, Rouprêt M, Le Cossec C, Granger B, Comperat E, de Gorski A, et al. First round of targeted biopsies with magnetic resonance imaging/ultrasound-fusion images compared to conventional ultrasound-guided trans-rectal biopsies for the diagnosis of localised prostate cancer. *BJU Int* 2014:Epub ahead of print., doi:10.1111/bju.12690.
 154. Sonn GA, Chang E, Natarajan S, Margolis DJ, Macairan M, Lieu P, et al. Value of targeted prostate biopsy using magnetic resonance-ultrasound fusion in men with prior negative biopsy and elevated prostate-specific antigen. *Eur Urol* 2014;65:809–15.
 155. Sonn GA, Natarajan S, Margolis DJ, MacAiran M, Lieu P, Huang J, et al. Targeted biopsy in the detection of prostate cancer using an office based magnetic resonance ultrasound fusion device. *J Urol* 2013;189:86–91.
 156. Kuru TH, Roethke MC, Seidenader J, Simpfendorfer T, Boxler S, Alammari K, et al. Critical evaluation of magnetic resonance imaging targeted, transrectal ultrasound guided transperineal fusion biopsy for detection of prostate cancer. *J Urol* 2013;190:1380–6.
 157. Engelhard K, Hollenbach HP, Kiefer B, Winkel A, Goeb K, Engehausen D. Prostate biopsy in the supine position in a standard 1.5-T scanner under real time MR-imaging control using a MR-compatible endorectal biopsy device. *Eur Radiol* 2006;16:1237–43.
 158. Franiel T, Stephan C, Erbersdobler A, Dietz E, Maxeiner A, Hell N, et al. Areas suspicious for prostate cancer: MR-guided biopsy in patients with at least one transrectal US-guided biopsy with a negative finding--multiparametric MR imaging for detection and biopsy planning. *Radiology* 2011;259:162–72.
 159. Hambrock T, Somford DM, Hoeks C, Bouwense S a W, Huisman H, Yakar D, et al. Magnetic resonance imaging guided prostate biopsy in men with repeat negative biopsies and increased prostate specific antigen. *J Urol* 2010;183:520–7.
 160. Hambrock T, Fütterer JJ, Huisman HJ, Hulsbergen-vandeKaa C, van Basten J-P, van Oort I, et al. Thirty-two-channel coil 3T magnetic resonance-guided biopsies of prostate tumor suspicious regions identified on multimodality 3T magnetic resonance imaging: technique and feasibility. *Invest Radiol* 2008;43:686–94.
 161. Roethke M, Anastasiadis A G, Lichy M, Werner M, Wagner P, Kruck S, et al. MRI-guided prostate biopsy detects clinically significant cancer: analysis of a cohort of 100 patients after previous negative TRUS biopsy. *World J Urol* 2012;30:213–8.
 162. Pokorny MR, de Rooij M, Duncan E, Schröder FH, Parkinson R, Barentsz JO, et al. Prospective Study of Diagnostic Accuracy Comparing Prostate Cancer Detection by Transrectal Ultrasound-Guided Biopsy Versus Magnetic Resonance (MR) Imaging with Subsequent MR-guided Biopsy in Men Without Previous Prostate Biopsies. *Eur Urol* 2014;1–8.
 163. Singh AK, Krieger A, Lattouf J-B, Guion P, Grubb RL, Albert PS, et al. Patient selection determines the prostate cancer yield of dynamic contrast-enhanced magnetic resonance imaging-guided transrectal biopsies in a closed 3-Tesla scanner. *BJU Int* 2008;101:181–5.
 164. Overduin CG, Fütterer JJ, Barentsz JO. MRI-guided biopsy for prostate cancer detection: a systematic review of current clinical results. *Curr Urol Rep* 2013;14:209–13.
 165. Beyersdorff D, Winkel A, Hamm B, Lenk S, Loening SA, Taupitz M. MR imaging-guided prostate biopsy with a closed MR unit at 1.5 T: initial results. *Radiology* 2005;234:576–81.
 166. Bratan F, Niaf E, Melodelima C, Chesnais AL, Souchon R, Mège-Lechevallier F, et al. Influence of imaging and histological factors on prostate cancer detection and localisation on multiparametric MRI: a prospective study. *Eur Radiol* 2013;23:2019–29.
 167. Vargas HA, Akin O, Shukla-Dave A, Zhang J, Zakian KL, Zheng J, et al. Performance characteristics of MR imaging in the evaluation of clinically low-risk prostate cancer: a prospective study. *Radiology* 2012;265:478–87.
 168. Doo KW, Sung DJ, Park BJ, Kim MJ, Cho SB, Oh YW, et al. Detectability of low and intermediate or high risk prostate cancer with combined T2-weighted and diffusion-weighted MRI. *Eur Radiol* 2012;22:1812–9.
 169. Kirkham APS, Emberton M, Allen C. How good is MRI at detecting and characterising cancer within the prostate? *Eur Urol* 2006;50:1163–74; discussion 1175.
 170. Delongchamps NB, Rouanne M, Flam T, Beuvon F, Liberatore M, Zerbib M, et al. Multiparametric magnetic resonance imaging for the detection and localization of prostate cancer: combination of T2-weighted, dynamic contrast-enhanced and diffusion-weighted imaging. *BJU Int* 2011;107:1411–8.
 171. Makarov D V, Trock BJ, Humphreys EB, Mangold LA, Walsh PC, Epstein JI, et al. Updated nomogram to predict pathologic stage of prostate cancer given prostate-specific antigen level, clinical stage, and biopsy Gleason score (Partin tables) based on cases from 2000 to 2005. *Urology* 2007;69:1095–101.
 172. Ohori M, Kattan MW, Koh H, Maru N, Slawin KM, Shariat S, et al. Predicting the presence and side of extracapsular extension: a nomogram for staging prostate cancer. *J Urol* 2004;171:1844–9; discussion 1849.
 173. Kattan MW, Eastham JA, Wheeler TM, Maru N, Scardino PT, Erbersdobler A, et al. Counseling men with prostate cancer: a nomogram for predicting the presence of small, moderately differentiated, confined tumors. *J Urol* 2003;170:1792–7.
 174. Koh H, Kattan MW, Scardino PT, Suyama K, Maru N, Slawin K, et al. A nomogram to predict seminal vesicle invasion by the extent and location of cancer in systematic biopsy results. *J Urol* 2003;170:1203–8.
 175. Cagiannos I, Karakiewicz P, Eastham JA, Ohori M, Rabbani F, Gerigk C, et al. A preoperative nomogram identifying decreased risk of positive pelvic lymph nodes in patients with prostate cancer. *J Urol* 2003;170:1798–803.
 176. Stephenson AJ, Kattan MW, Eastham JA, Bianco FJ, Yossepowitch O, Vickers AJ, et al. Prostate cancer-specific mortality after radical prostatectomy for patients treated in the prostate-specific antigen era. *J Clin Oncol* 2009;27:4300–5.
 177. Stephenson AJ, Scardino PT, Eastham JA, Bianco FJ, Dotan ZA, DiBlasio CJ, et al. Postoperative nomogram predicting

- the 10-year probability of prostate cancer recurrence after radical prostatectomy. *J Clin Oncol* 2005;23:7005–12.
178. Thörmer G, Otto J, Horn L-C, Garnov N, Do M, Franz T, et al. Non-invasive estimation of prostate cancer aggressiveness using diffusion-weighted MRI and 3D proton MR spectroscopy at 3.0 T. *Acta Radiol* 2014:Epub ahead of print., doi:10.1177/028418511352031.
 179. Lebovici A, Sfrangeu SA, Feier D, Caraiani C, Lucan C, Suciu M, et al. Evaluation of the normal-to-diseased apparent diffusion coefficient ratio as an indicator of prostate cancer aggressiveness. *BMC Med Imaging* 2014;14:15.
 180. Rosenkrantz AB, Kopec M, Kong X, Melamed J, Dakwar G, Babb JS, et al. Prostate cancer vs. post-biopsy hemorrhage: diagnosis with T2- and diffusion-weighted imaging. *J Magn Reson Imaging* 2010;31:1387–94.
 181. Watanabe Y, Terai A, Araki T, Nagayama M, Okumura A, Amoh Y, et al. Detection and localization of prostate cancer with the targeted biopsy strategy based on ADC map: a prospective large-scale cohort study. *J Magn Reson Imaging* 2012;35:1414–21.
 182. Donati OF, Mazaheri Y, Afaq A, Vargas HA, Zheng J, Moskowitz CS, et al. Prostate cancer aggressiveness: assessment with whole-lesion histogram analysis of the apparent diffusion coefficient. *Radiology* 2014;271:143–52.
 183. Moore CM, Ridout A, Emberton M. The role of MRI in active surveillance of prostate cancer. *Curr Opin Urol* 2013;23:261–7.
 184. Hu JC, Chang E, Natarajan S, Margolis DJ, Macairan M, Lieu P, et al. Targeted prostate biopsy in select men for active surveillance-do the epstein criteria still apply? *J Urol* 2014;192:385–90.
 185. Somford DM, Hoeks CM, Hulsbergen-van de Kaa CA, Hambroek T, Fütterer JJ, Witjes JA, et al. Evaluation of diffusion-weighted MR imaging at inclusion in an active surveillance protocol for low-risk prostate cancer. *Invest Radiol* 2013;48:152–7.
 186. Hoeks CM, Somford DM, van Oort IM, Vergunst H, Oddens JR, Smits GA, et al. Value of 3-T Multiparametric Magnetic Resonance Imaging and Magnetic Resonance-Guided Biopsy for Early Risk Re-stratification in Active Surveillance of Low-Risk Prostate Cancer: A Prospective Multicenter Cohort Study. *Invest Radiol* 2013;49:165–72.
 187. Shukla-Dave A, Hricak H, Akin O, Yu C, Zakian KL, Udo K, et al. Preoperative nomograms incorporating magnetic resonance imaging and spectroscopy for prediction of insignificant prostate cancer. *BJU Int* 2012;109:1315–22.
 188. Duffield AS, Lee TK, Miyamoto H, Carter HB, Epstein JI. Radical prostatectomy findings in patients in whom active surveillance of prostate cancer fails. *J Urol* 2009;182:2274–8.
 189. Bangma CH, Bul M, van der Kwast TH, Pickles T, Korfage IJ, Hoeks CM, et al. Active surveillance for low-risk prostate cancer. *Crit Rev Oncol Hematol* 2013;85:295–302.
 190. Huang CC, Kong MX, Zhou M, Rosenkrantz AB, Taneja SS, Melamed J, et al. Gleason Score 3 + 4=7 Prostate Cancer With Minimal Quantity of Gleason Pattern 4 on Needle Biopsy Is Associated With Low-risk Tumor in Radical Prostatectomy Specimen. *Am J Surg Pathol* 2014;38(8):1096–101.
 191. Soulié M. What is the Role of Surgery for Locally Advanced Disease? *Eur Urol Suppl* 2008;7:400–5.
 192. Fütterer JJ, Heijmink SWTPJ, Scheenen TWJ, Jager GJ, Hulsbergen-Van de Kaa CA, Witjes JA, et al. Prostate cancer: local staging at 3-T endorectal MR imaging--early experience. *Radiology* 2006;238:184–91.
 193. Villers A, Puech P, Mouton D, Leroy X, Ballereau C, Lemaitre L. Dynamic contrast enhanced, pelvic phased array magnetic resonance imaging of localized prostate cancer for predicting tumor volume: correlation with radical prostatectomy findings. *J Urol* 2006;176:2432–7.
 194. Turkbey B, Mani H, Aras O, Rastinehad AR, Shah V, Bernardo M, et al. Correlation of magnetic resonance imaging tumor volume with histopathology. *J Urol* 2012;188:1157–63.
 195. Girouin N, Mège-Lechevallier F, Tonina Senes A, Bissery A, Rabilloud M, Maréchal J-M, et al. Prostate dynamic contrast-enhanced MRI with simple visual diagnostic criteria: is it reasonable? *Eur Radiol* 2007;17:1498–509.
 196. Noguchi M, Stamey TA, McNeal JE, Nolley R. Prognostic factors for multifocal prostate cancer in radical prostatectomy specimens: lack of significance of secondary cancers. *J Urol* 2003;170:459–63.
 197. Wise AM, Stamey TA, McNeal JE, Clayton JL. Morphologic and clinical significance of multifocal prostate cancers in radical prostatectomy specimens. *Urology* 2002;60:264–9.
 198. Wang L. Incremental value of magnetic resonance imaging in the advanced management of prostate cancer. *World J Radiol* 2009;1:3–14.
 199. Somford DM, Hamoen EH, Fütterer JJ, van Basten JP, Hulsbergen-van de Kaa CA, Vreuls W, et al. The predictive value of endorectal 3 Tesla multiparametric magnetic resonance imaging for extraprostatic extension in patients with low, intermediate and high risk prostate cancer. *J Urol* 2013;190:1728–34.
 200. Augustin H, Fritz G a, Ehammer T, Auprich M, Pummer K. Accuracy of 3-Tesla magnetic resonance imaging for the staging of prostate cancer in comparison to the Partin tables. *Acta Radiol* 2009;50:562–9.
 201. Gupta RT, Faridi KF, Singh AA, Passoni NM, Garcia-Reyes K, Madden JF, et al. Comparing 3-T multiparametric MRI and the Partin tables to predict organ-confined prostate cancer after radical prostatectomy. *Urol Oncol* 2014:Epub ahead of print., doi:10.1016/j.urolonc.2014.
 202. Ren J, Huan Y, Wang H, Ge Y, Chang Y, Yin H, et al. Seminal vesicle invasion in prostate cancer: prediction with combined T2-weighted and diffusion-weighted MR imaging. *Eur Radiol* 2009;19:2481–6.
 203. Kim CK, Choi D, Park BK, Kwon GY, Lim HK. Diffusion-weighted MR imaging for the evaluation of seminal vesicle invasion in prostate cancer: initial results. *J Magn Reson Imaging* 2008;28:963–9.
 204. Park BH, Jeon HG, Jeong BC, Seo S II, Lee HM, Choi HY, et al. Influence of Magnetic Resonance Imaging in the Decision to Preserve or Resect Neurovascular Bundles at Robotic Assisted Laparoscopic Radical Prostatectomy. *J Urol* 2014:Epub ahead of print., doi:10.1016/j.juro.2014.01.
 205. Panebianco V, Salciccia S, Cattarino S, Minisola F, Gentilucci A, Alfarone A, et al. Use of Multiparametric MR with Neurovascular Bundle Evaluation to Optimize the Oncological and Functional Management of Patients Considered for Nerve-Sparing Radical Prostatectomy. *J Sex Med* 2012;2157–66.
 206. Dickinson L, Ahmed HU, Allen C, Barentsz JO, Carey B, Fütterer JJ, et al. Scoring systems used for the interpretation and reporting of multiparametric MRI for prostate cancer detection, localization, and characterization: could standardization lead to improved utilization of imaging

- within the diagnostic pathway? *J Magn Reson Imaging* 2013;37:48–58.
207. Junker D, Schäfer G, Edlinger M, Kremser C, Bektic J, Horninger W, et al. Evaluation of the PI-RADS scoring system for classifying mpMRI findings in men with suspicion of prostate cancer. *Biomed Res Int* 2013;doi: 10.1155/2013/252939.
 208. Langer DL, van der Kwast TH, Evans AJ, Trachtenberg J, Wilson BC, Haider MA. Prostate cancer detection with multi-parametric MRI: logistic regression analysis of quantitative T2, diffusion-weighted imaging, and dynamic contrast-enhanced MRI. *J Magn Reson Imaging* 2009;30:327–34.
 209. Hansford BG, Karademir I, Peng Y, Jiang Y, Karczmar G, Thomas S, et al. Dynamic contrast-enhanced MR imaging features of the normal central zone of the prostate. *Acad Radiol* 2014;21:569–77.
 210. Ward JF, Slezak JM, Blute ML, Bergstralh EJ, Zincke H. Radical prostatectomy for clinically advanced (cT3) prostate cancer since the advent of prostate-specific antigen testing: 15-year outcome. *BJU Int* 2005;95:751–6.
 211. Hsu C-Y, Joniau S, Oyen R, Roskams T, Van Poppel H. Outcome of surgery for clinical unilateral T3a prostate cancer: a single-institution experience. *Eur Urol* 2007;51:121–8; discussion 128–9.
 212. Mitchell CR, Boorjian S a, Umbreit EC, Rangel LJ, Carlson RE, Karnes RJ. 20-Year survival after radical prostatectomy as initial treatment for cT3 prostate cancer. *BJU Int* 2012;110:1709–13.
 213. Spahn M, Briganti A, Capitanio U, Kneitz B, Gontero P, Karnes JR, et al. Outcome predictors of radical prostatectomy followed by adjuvant androgen deprivation in patients with clinical high risk prostate cancer and pT3 surgical margin positive disease. *J Urol* 2012;188:84–90.
 214. Ruprecht O, Weisser P, Bodelle B, Ackermann H, Vogl TJ. MRI of the prostate: interobserver agreement compared with histopathologic outcome after radical prostatectomy. *Eur J Radiol* 2012;81:456–60.
 215. Garcia-Reyes K, Passoni NM, Palmeri ML, Kauffman CR, Choudhury KR, Polascik TJ, et al. Detection of prostate cancer with multiparametric MRI (mpMRI): effect of dedicated reader education on accuracy and confidence of index and anterior cancer diagnosis. *Abdom Imaging* 2014;Epub ahead of print., doi: 10.1007/s00261-014-019.
 216. Beyersdorff D, Taymoorian K, Knösel T, Schnorr D, Felix R, Hamm B, et al. MRI of prostate cancer at 1.5 and 3.0 T: comparison of image quality in tumor detection and staging. *AJR Am J Roentgenol* 2005;185:1214–20.
 217. Qayyum A, Coakley F V, Lu Y, Olpin JD, Wu L, Yeh BM, et al. Organ-confined prostate cancer: effect of prior transrectal biopsy on endorectal MRI and MR spectroscopic imaging. *AJR Am J Roentgenol* 2004;183:1079–83.
 218. Park KK, Lee SH, Lim BJ, Kim JH, Chung BH. The effects of the period between biopsy and diffusion-weighted magnetic resonance imaging on cancer staging in localized prostate cancer. *BJU Int* 2010;106:1148–51.
 219. Puech P, Rouvière O, Renard-Penna R, Villers A, Devos P, Colombel M, et al. Prostate cancer diagnosis: multiparametric MR-targeted biopsy with cognitive and transrectal US-MR fusion guidance versus systematic biopsy--prospective multicenter study. *Radiology* 2013;268:461–9.
 220. Wysock JS, Rosenkrantz AB, Huang WC, Stifelman MD, Lepor H, Deng F-M, et al. A Prospective, Blinded Comparison of Magnetic Resonance (MR) Imaging-Ultrasound Fusion and Visual Estimation in the Performance of MR-targeted Prostate Biopsy: The PROFUS Trial. *Eur Urol* 2013;Epub ahead of print., doi:10.1016/j.eururo.2013.1.
 221. Ahmed HU, Kirkham A, Arya M, Illing R, Freeman A, Allen C, et al. Is it time to consider a role for MRI before prostate biopsy? *Nat Rev Clin Oncol* 2009;6:197–206.
 222. Numao N, Yoshida S, Komai Y, Ishii C, Kagawa M, Kijima T, et al. Usefulness of pre-biopsy multiparametric magnetic resonance imaging and clinical variables to reduce initial prostate biopsy in men with suspected clinically localized prostate cancer. *J Urol* 2013;190:502–8.
 223. Tombal B. Toward the end of blind prostate biopsies? *Eur Urol* 2012;62:997–8; discussion 999–1000.
 224. De Rooij M, Crienien S, Witjes JA, Barentsz JO, Rovers MM, Grutters JPC. Cost-effectiveness of Magnetic Resonance (MR) Imaging and MR-guided Targeted Biopsy Versus Systematic Transrectal Ultrasound-Guided Biopsy in Diagnosing Prostate Cancer: A Modelling Study from a Health Care Perspective. *Eur Urol* 2013;1–7.
 225. Vargas HA, Akin O, Afaq A, Goldman D, Zheng J, Moskowitz CS, et al. Magnetic resonance imaging for predicting prostate biopsy findings in patients considered for active surveillance of clinically low risk prostate cancer. *J Urol* 2012;188:1732–8.
 226. Margel D, Yap SA, Lawrentschuk N, Klotz L, Haider M, Hersey K, et al. Impact of multiparametric endorectal coil prostate magnetic resonance imaging on disease reclassification among active surveillance candidates: a prospective cohort study. *J Urol* 2012;187:1247–52.
 227. Kasivisvanathan V, Dufour R, Moore CM, Ahmed HU, Abd-Alazeez M, Charman SC, et al. Transperineal magnetic resonance image targeted prostate biopsy versus transperineal template prostate biopsy in the detection of clinically significant prostate cancer. *J Urol* 2013;189:860–6.
 228. Park BH, Jeon HG, Jeong BC, Seo S II, Lee HM, Choi HY, et al. Role of multiparametric 3.0 tesla magnetic resonance imaging for decision-making to preserve or resect neurovascular bundles at robotic assisted laparoscopic radical prostatectomy. *J Urol* 2014.
 229. Stamatakis L, Siddiqui MM, Nix JW, Logan J, Rais-Bahrami S, Walton-Diaz A, et al. Accuracy of multiparametric magnetic resonance imaging in confirming eligibility for active surveillance for men with prostate cancer. *Cancer* 2013;119:3359–66.